Gdański Uniwersytet Medyczny

Wydział Nauk o Zdrowiu

Rozprawa doktorska

Analiza teksturalna obrazów rezonansu magnetycznego jako potencjalne narzędzie diagnostyczne

Textural analysis of magnetic resonance imaging as a potential diagnostic tool

mgr Małgorzata Grzywińska

Zakład Neurofizjologii, Neuropsychologii i Neuroinformatyki
Gdańskiego Uniwersytetu Medycznego

Promotor: prof. dr hab. Paweł Winklewski
Zakład Neurofizjologii, Neuropsychologii i Neuroinformatyki
Gdańskiego Uniwersytetu Medycznego

Promotor pomocniczy: dr n. med. Dominik Świętoń
II Zakład Radiologii
Gdańskiego Uniwersytetu Medycznego

Gdańsk 2024

Wyrażam głęboką wdzięczność

Profesorowi dr. hab. Pawłowi Winklewskiemu, mojemu promotorowi,
oraz doktorowi n. med. Dominikowi Świętoniowi, mojemu promotorowi pomocniczemu,
za ich bezgraniczną cierpliwość i nieocenione wsparcie na mojej ścieżce naukowej.

Autorom,
którzy współtworzyli artykuły włączone do mojej rozprawy doktorskiej,
za inspirującą i owocną współpracę.

Rodzinie i Przyjaciołom,
za nieustające wsparcie i wiarę we mnie.

SPIS TREŚCI

WYKAZ PRAC WCHODZĄCYCH W SKŁAD ROZPRAWY DOKTORSKIEJ / LIST OF MANUSCRIPTS INCLUDED IN THE DOCTORAL DISSERTATION

Grzywińska Małgorzata, Jankowska Magdalena, Banach-Ambroziak Ewa, Szurowska Edyta, Dębska-Ślizień Alicja

Computation of the texture features on T2-weighted images as a novel method to assess the function of the transplanted kidney: primary research.

Transplant. Proc., 2020: vol. 52, nr 7, s. 2062-2066

DOI: 10.1016/j.transproceed.2020.02.084

IF 1.066 | MNiSW: 40 pkt | praca oryginalna

Grzywińska Małgorzata, Karwecka Magdalena, Pomorska Anna, Irga-Jaworska Ninela, Świętoń Dominik

Textural analysis of magnetic resonance images as an additional evaluation tool of parotid glands in Sjögren - primarily findings

Biomedicines, 2023 : vol. 11, nr 12, art. ID 3132, s. 1-12

DOI: 10.3390/biomedicines11123132

IF 4.700 | MNiSW: 100 pkt | praca oryginalna

SŁOWA KLUCZOWE / KEY WORDS

Analiza teksturalna, obrazowanie rezonansem magnetycznym (MRI), zespół Sjögrena, funkcja przeszczepionej nerki, nieinwazyjna diagnostyka, cechy tekstury MRI, pyradiomika, monitorowanie choroby, ocena zapalna, zmiany mikrostrukturalne, ocena kliniczna, techniki obrazowania diagnostycznego

Textural analysis, Magnetic Resonance Imaging (MRI), Sjogren's syndrome, transplanted kidney function, non-invasive diagnosis, MRI texture features, pyradiomics, disease monitoring, inflammatory grading, microstructural changes, clinical evaluation, diagnostic imaging techniques

STRESZCZENIE W JĘZYKU POLSKIM

1. WYKAZ STOSOWANYCH SKRÓTÓW

BMI	Wskaźnik Masy Ciała
CKD	Przewlekła Choroba Nerek
eGFR	Szacunkowy Wskaźnik Filtracji Kłębuszkowej
MDRD	Szacunkowy Wskaźnik Filtracji Kłębuszkowej (uproszczony)
CKD	Przewlekła choroba nerek
TSE	Turbo Spin Echo
SPAIR	Spektralne Wstępne Nasycenie z Odwróceniem
3D TSE SPIR imaging	Obrazowanie 3D Turbo Spin Echo Spektralne Wstępne Nasycenie z Odwróceniem
mDixon	Pozyskiwanie obrazów echa gradientowego w fazie i przeciwfazie
STIR	Krótki Odwrócony Czas Relaksacji
T2	Stała czasowa dla rozpadu/dekoherencji magnetyzacji poprzecznej
DWI	Obrazowanie Dyfuzyjne
ADC	Pozorny współczynnik dyfuzji
ROI	Region Zainteresowania
FSO	Statystyka Pierwszego Rzędu
GLCM	Macierz Współwystępowania Poziomów Szarości
GLSZM	Macierz Rozmiaru Stref Poziomów Szarości
GLRLM	Macierz Długości Ciągów Poziomów Szarości
NGTDM	Macierz Różnic Tonów Szarości Sąsiedztwa
GLDM	Macierz Zależności Poziomów Szarości
SAE	Podkreślenie Małych Obszarów
LAE	Podkreślenie Dużych Obszaró®
GLN	Niejednorodność Poziomów Szarości
GLNN	Normalizowana Niejednorodność Poziomów Szarości
SZN	Niejednorodność Stref Rozmiaru
SZNN	Normalizowana Niejednorodność Stref Rozmiaru
ZP	Procent Strefy
GLV	Wariancja Poziomów Szarości
ZV	Wariancja Strefy
ZE	Entropia Strefy
LGLZE	Podkreślenie Strefy Niskich Poziomów Szarości
HGLZE	Podkreślenie Strefy Wysokich Poziomów Szarości
SALGLE	Podkreślenie Małe Obszary Niskich Poziomów Szarości
SAHGLE	Podkreślenie Małe Obszary Wysokich Poziomów Szarości
LALGLE	Podkreślenie Duże Obszary Niskich Poziomów Szarości
LAHGLE	Podkreślenie Duże Obszary Wysokich Poziomów Szarości
SRE	Podkreślenie Krótkich Ciągiów
LRE	Podkreślenie Długich Ciągiów
RLN	Niejednorodność Długości Ciągów
RLNN	Normalizowana Niejednorodność Długości Ciągów
RP	Procent Ciągu
RV	Wariancja Ciągu
RE	Entropia Ciągu
LGLRE	Podkreślenie Ciągiów Niskich Poziomów Szarości
HGLRE	Podkreślenie Ciągiów Wysokich Poziomów Szarości

SRLGLE	Podkreślenie Krótkich Ciągiów Niskich Poziomów Szarości
SRHGLE	Podkreślenie Krótkich Ciągiów Wysokich Poziomów Szarości
LRLGLE	Podkreślenie Długich Ciągiów Niskich Poziomów Szarości
LRHGLE	Podkreślenie Długich Ciągiów Wysokich Poziomów Szarości
SDE	Podkreślenie Małej Zależności
LDE	Podkreślenie Dużej Zależności
DN	Niejednorodność Zależności
DNN	Normalizowana Niejednorodność Zależności
DV	Wariancja Zależności
DE	Entropia Zależności
LGLE	Podkreślenie Niskich Poziomów Szarości
HGLE	Podkreślenie Wysokich Poziomów Szarości
SDLGLE	Podkreślenie Małej Zależności Niskich Poziomów Szarości
SDHGLE	Podkreślenie Małej Zależności Wysokich Poziomów Szarości
LDLGLE	Podkreślenie Dużej Zależności Niskich Poziomów Szarości
LDHGLE	Podkreślenie Dużej Zależności Wysokich Poziomów Szarości

2. WPROWADZENIE

Analiza teksturalna, stosowana w diagnostyce obrazowej, zwłaszcza w rezonansie magnetycznym (MRI), jest innowacyjną techniką, która może zmienić sposób, w jaki lekarze postrzegają i interpretują obrazy medyczne. Wykorzystując zaawansowane algorytmy do analizy szczegółów tekstury, metoda ta umożliwia wydobycie informacji z obrazów, pozwalając lekarzom na lepsze zrozumienie procesów zachodzących w mikrostrukturach tkankowych. Ta subtelna analiza wykracza poza możliwości tradycyjnych technik obrazowania, umożliwiając wykrycie zmian na poziomie molekularnym i tkankowym, które mogą być kluczowe dla wczesnego rozpoznawania, monitorowania oraz leczenia różnych jednostek chorobowych.

Tekstura obrazu MRI, rozumiana jako złożony wzorzec intensywności wokseli, może ujawnić istotne informacje o składzie, strukturze oraz funkcji tkanki. Analiza teksturalna wykorzystuje parametry między innymi takie jak kontrast, jednorodność czy entropia do oceny i interpretacji tych wzorców, co pozwala na identyfikację subtelnych różnic w obrazach tkankowych, często niewidocznych dla standardowych metod obrazowania.

W dziedzinie onkologii, gdzie wczesne wykrycie i monitorowanie reakcji na terapię ma kluczowe znaczenie, analiza teksturalna może stać się nieocenionym narzędziem. Pozwolić może na identyfikację mikroskopijnych zmian w tkance nowotworowej, które mogą wskazywać na odpowiedź na leczenie lub jej brak, jeszcze zanim będą widoczne jakiekolwiek zmiany w rozmiarze guza. To z kolei może umożliwić lekarzom szybką modyfikację planu terapii, zwiększając tym samym szanse pacjenta na powrót do zdrowia.

Co więcej, analiza teksturalna może odegrać kluczową rolę w personalizowanej medycynie. Poprzez możliwą identyfikację unikalnych wzorców teksturalnych, związanych z określonymi stanami patologicznymi, lekarze będą mogli dostosować terapię do indywidualnych cech choroby pacjenta, co może znacząco poprawić efektywność leczenia. Personalizacja terapii, oparta na precyzyjnej diagnozie, staje się dzięki temu bardziej osiągalna, co stanowi ogromny postęp w medycynie, przyczyniając się do zwiększenia szans na sukces terapeutyczny.

Bezpieczeństwo i komfort pacjenta są kolejnymi ważnymi aspektami, gdzie analiza teksturalna ma znaczący wpływ. Jako metoda nieinwazyjna używająca obrazy, które pacjent rutynowo uzyskuje w trakcie diagnostyki, znacząco może ograniczyć ryzyko powikłań związanych z inwazyjnymi procedurami diagnostycznymi. To może uczynić ją szczególnie wartościową w przypadkach, gdzie konieczne jest częste monitorowanie stanu pacjenta, jak na przykład w przypadku chorób przewlekłych czy w onkologii. Ponadto, nieinwazyjny charakter analizy teksturalnej może sprawić, że jest ona metodą bezpieczną i przyjazną dla pacjentów, w tym dla dzieci oraz osób z grup wysokiego ryzyka.

Kolejnym przykładem może być istotność tej metody w neurologii, analiza teksturalna również odgrywać może tu kluczową rolę, umożliwiając lepsze zrozumienie mechanizmów chorób neurodegeneracyjnych. Przez analizę subtelnych zmian w strukturze mózgu, lekarze będą mogli lepiej zrozumieć, jak choroby takie jak Alzheimer czy stwardnienie rozsiane wpływają na tkankę mózgową, co może prowadzić do wcześniejszego rozpoznania i lepszego dostosowania terapii.

Podsumowując, analiza teksturalna w diagnostyce obrazowej jest przełomem technologicznym, który znacząco może poszerzyć możliwości diagnostyczne i terapeutyczne w medycynie. Oferuje ona możliwość nie tylko wczesnego wykrywania chorób i możliwe precyzyjne monitorowanie leczenia, ale również może otworzyć drogę do bardziej spersonalizowanej i skutecznej opieki medycznej. Przez umożliwienie lekarzom głębszego zrozumienia subtelnych zmian tkankowych, analiza teksturalna może przyczynić się do szybszego i bardziej świadomego podejmowania decyzji klinicznych, co z kolei może przełożyć się na lepsze wyniki leczenia i poprawę jakości życia pacjentów. W erze, gdzie precyzja i personalizacja w medycynie stają się coraz bardziej pożądane, analiza teksturalna wyróżnia się jako kluczowe narzędzie, wspierające rozwój nowoczesnej, skoncentrowanej na pacjencie opieki zdrowotnej.

3. CELE PRACY

Podstawowym celem badań było eksploracja i zweryfikowanie Analizy Teksturalnej (TA) jako narzędzia wspomagającego w diagnostyce i monitoringu stanu zdrowia za pomocą Obrazowania Rezonansem Magnetycznym (MRI). Konkretnie, te badania miały na celu udoskonalenie i potwierdzenie TA jako metody uzupełniającej tradycyjne podejścia diagnostyczne, poprawiając dokładność diagnozowania i monitorowania stanu zdrowia pacjentów, co przekłada się na większą precyzję i efektywność diagnostyki.

1. Pierwszy Artykuł:

   Cel: Ocena potencjalnej roli TA w monitorowaniu funkcji przeszczepionych nerek.

   Cel szczegółowy: Prezentacja TA jako metody umożliwiającej identyfikację zależności między parametrami tekstury a wskaźnikami funkcji nerek (takimi jak eGFR i kreatynina).

2. Drugi Artykuł:

   Cel: Eksploracja możliwości zastosowania TA w ocenie stanu gruczołów ślinowych w kontekście zespołu Sjögrena u dzieci.

   Cel szczegółowy: Demonstracja, że TA może służyć jako narzędzie do nieinwazyjnej oceny i potencjalnego różnicowania stanów patologicznych gruczołów ślinowych, co może być szczególnie wartościowe w diagnostyce zespołu Sjögrena.

Podsumowując, nadrzędnym celem jest rozwój i potwierdzenie skuteczności TA jako narzędzia wspomagającego standardowe metody MRI, z nadzieją na ulepszenie diagnostyki i monitorowania stanu zdrowia bez konieczności stosowania dodatkowych inwazyjnych procedur. Oba artykuły podkreślają potrzebę dalszych badań w celu dokładnego zrozumienia możliwości, ograniczeń i praktycznego zastosowania TA w medycynie klinicznej. Wskazują one na potencjał TA jako narzędzia uzupełniającego standardowe metody MRI, z nadzieją na ulepszenie procesów diagnostycznych i monitorowania stanu zdrowia, jednocześnie zaznaczając, że dalsze badania są konieczne, aby w pełni wykorzystać możliwości TA.

4. OMÓWIENIE PUBLIKACJI WCHODZĄCYCH W SKŁAD ROZPRAWY DOKTORSKIEJ

1. Publikacja 1.

Computation of the texture features on T2-weighted images as a novel method to assess the function of the transplanted kidney: primary research.

Celem badania było zastosowanie analizy teksturalnej (TA) do oceny funkcji nerek po transplantacji (KTx). Przeprowadzone badania opierają się na hipotezie, że TA stosowana do obrazów MRI z ważeniem T2 może skutecznie ocenić funkcję przeszczepionych nerek. W publikacji przeanalizowano cechy teksturalne obrazów z ważeniem T2 od dziewięciu pacjentów z przeszczepionymi nerkami, dążąc do wykrycia statystycznej różnicy w tych cechach w zależności od umiejscowienia regionu zainteresowania (ROI) w obrębie nerek.

Metodologia badania obejmuje retrospektywne badania skanów MRI wybranych pacjentów. Szczególne znaczenie ma skupienie się na obrazach z ważeniem T2, biorąc pod uwagę ich istotność w obrazowaniu nerek. W badaniu zanalizowano cechy teksturalne i korelacje tych cech z oszacowaną czynnościową filtracją kłębuszkową (eGFR), obliczaną przy użyciu formuły Chronic Kidney Disease Epidemiology Collaboration (CKD-EPI). Do analizy statystycznej wykorzystywano test korelacji Spearmana i test U Manna-Whitneya.

Zaobserwowano znaczącą korelację między parametrami teksturalnymi obrazów z ważeniem T2 a wskaźnikami funkcji nerek, głównie eGFR i poziomami kreatyniny. Korelacja ta jest szczególnie wyraźna, gdy ROI znajduje się w korze nerki, co sugeruje, że cechy teksturalne regionu korowego lepiej opisują funkcję nerki niż te z regionu piramid. Wykazano znaczące różnice w parametrach teksturalnych w zależności od umiejscowienia ROI, potwierdzając hipotezę, że przestrzenny rozkład ROI w obrębie nerki wpływa na wyniki analizy teksturalnej.

Artykuł odnosi się do znaczenia wyżej wymienionych zależności. Znacząca korelacja między określonymi parametrami teksturalnymi a wskaźnikami funkcji nerek, szczególnie w regionie korowym, podkreśla potencjał TA w nieinwazyjnym monitorowaniu zdrowia i funkcji przeszczepionych nerek. Brak znaczącej korelacji między cechami teksturalnymi a wskaźnikami funkcji nerek przy rozważaniu całego ROI nerki jest intrygującym odkryciem, podkreślającym złożoność struktury i funkcji nerek oraz potrzebę precyzyjnego umiejscowienia ROI w TA.

Zastosowanie obrazów MRI z T2 do analizy teksturalnej jest nową i potencjalnie rozwojową metodą oceny funkcji przeszczepionych nerek. Znaczące korelacje zaobserwowane między parametrami teksturalnymi a kluczowymi wskaźnikami funkcji nerek, szczególnie w korze nerki, otwierają nową drogę dla nieinwazyjnego, obrazowego monitorowania biorców przeszczepów nerek. W publikacji wskazano również potrzebę dalszych badań, zwłaszcza w celu określenia optymalnej wielkości ROI i jego umiejscowienia w obrębie narządu, aby w pełni wykorzystać potencjał TA w tym kontekście.

Podsumowując, badanie przedstawia możliwość wykorzystania analizy teksturalnej obrazów MRI z ważeniem T2 do oceny funkcji przeszczepionych nerek. Zaobserwowana korelacja między parametrami teksturalnymi a wskaźnikami funkcji nerek może otwierać nowe możliwości nieinwazyjnego monitorowania przeszczepów nerek. Niemniej jednak, w publikacji również wskazuje na potrzebę dalszych kompleksowych badań w celu udoskonalenia metodologii i wykorzystania w pełni potencjału tej innowacyjnej metody.

2. Publikacja 2.

Textural analysis of magnetic resonance images as an additional evaluation tool of parotid glands in Sjögren - primarily findings

Zespół Sjögrena (SS) u pacjentów pediatrycznych stwarza unikalne wyzwania diagnostyczne z powodu swojej niespecyficznej i często opóźnionej prezentacji klinicznej. Tradycyjne metody diagnostyczne, takie jak ultrasonografia gruczołów ślinowych, sialografia i scyntygrafia, dostarczają cennych informacji, ale wiążą się z istotnymi ograniczeniami i ryzykiem. Sialografia MRI jest niedostatecznie wykorzystywana, a analiza tekstury obrazów MRI jest obiecującą metodą, która może ulepszyć proces diagnostyczny.

Badanie objęło 36 pacjentów z dodatnim wynikiem biopsji przyusznych gruczołów ślinowych dla SS oraz grupę kontrolną 20 ochotników w wieku od 5 roku życia do 20 roku życia. Protokół badania obejmował sekwencję przeglądową i sekwencje morfologiczne w trzech płaszczyznach. Główne sekwencje to obrazowanie z ważeniem dyfuzyjnym (DWI) oraz obrazowanie z ważeniem T2, które umożliwiały wszechstronną ocenę aspektów anatomicznych i patologicznych odgrywając kluczową rolę w zrozumieniu zespołu Sjögrena w populacji pediatrycznej.

Ocenę stanu gruczołów ślinowych przeprowadzono na podstawie zmodyfikowanych kryteriów Tonami. Ocena była oparta na wysokiej intensywności sygnału T2 w całym obszarze gruczołów w sekwencji sialografii MRI. Do korekty niejednorodności pola zastosowano algorytm N4, zwiększając tym samym jakość i dokładność analizy. Aby zminimalizować potencjalny wpływ otaczających tkanek lub artefaktów, obszar zainteresowania (ROI) został ręcznie nakreślony tak, aby obejmował wszystkie gruczoły, z marginesem 1 mm od krawędzi.

Cechy tekstury ekstrahowane z ROI zostały podzielone na podgrupy: statystyki pierwszego rzędu, macierz współwystępowania poziomów szarości, macierz rozmiaru strefy szarości, macierz długości biegu szarości, macierz różnicy tonów szarości sąsiednich oraz macierz zależności poziomu szarości. Analizy statystyczne przeprowadzono za pomocą SPSS Statistics 27. Test Shapiro-Wilka ujawnił, że parametry nie podążały za normalnym rozkładem, co skłoniło do zastosowania testu korelacji Spearmana w celu zbadania relacji między zebranymi danymi oraz zidentyfikowania korelacji między cechami tekstury w chorych i zdrowych gruczołach. Test Kruskala-Wallisa dla niezależnych prób został zastosowany do porównania różnic grupowych między gruczołami, a analiza post hoc przeprowadzona została w celu określenia, które grupy wykazały istotne różnice, przyjmując poziom istotności na $p<0,05$.

W badaniu oceniono stopnie sialografii MRI dla każdego gruczołu, biorąc pod uwagę obecność zmian torbielowatych. Zanotowano następujący rozkład: stopień 0 w 12 gruczołach (16%), stopień 1 w 8 gruczołach (11%), stopień 2 w 30 gruczołach (42%) i stopień 3 w 22 gruczołach (31%). Średnia wartość współczynnika dyfuzji (ADC) dla pacjentów z SS i grupy kontrolnej została uzyskana z ROI w każdym gruczole, przy czym średnia wartość ADC była zależna od stopnia morfologii MRI. Stwierdzono statystycznie istotne różnice ($p<0,05$) między grupami: 1 - zdrowe ($p= 0,005$), 1-3 ($p=0,046$), 0 - 3 ($p=0,035$) oraz 0 - zdrowe ($p=0,001$). Całkowite obrazy ADC do analizy tekstury zostały wygenerowane dla każdego gruczołu, bez rozróżnienia między gruczołami lewymi a prawymi. Znaleziono umiarkowaną korelację między cechami

tekstury a stopniami morfologii MRI, a konkretnie zauważono pozytywną i umiarkowaną korelację między indywidualnymi parametrami morfologii MRI a niektórymi konkretnymi parametrami tekstury, szczególnie parametrami statystyk pierwszego rzędu. Ta korelacja sugeruje, że parametry statystyk pierwszego rzędu mogą zostać wykorzystane do skutecznego wyodrębniania kluczowych szczegółów dotyczących cech strukturalnych gruczołu, jak widać na obrazach MRI.

W badaniu porównano również średnie wartości analizy obrazu i tekstury obrazów ADC z ocenami MRI w klasyfikacji Tonami. Parametry obejmowały skalę Tonami, entropię, kurtozę, skośność, GLDM_Zależność od Niejednorodności, GLDM_Mała Zależność Wysokiego Poziomu Szarości, GLCM_Imc1, GLRLM_Entropia Biegu oraz GLSZM_Entropia Strefy. Wyniki wskazały, że wartości ADC były zbliżone do ocen MRI według. skali Tonami, co potwierdza średnia wynosząca 0.01, odchylenie standardowe 0.00 i kurtoza 3.86. Ponadto, GLDM_Zależność od Niejednorodności i GLDM_Mała Zależność Wysokiego Poziomu Szarości wykazały podobne wartości, wskazując na możliwość zastosowania obrazów ADC do wcześniejszego wykrywanie stopnia 1 w MRI w klasyfikacji Tonami.

Zbadano różnice teksturalne w dwóch regularnie pozyskiwanych sekwencjach MRI u pacjentów z SS - mapach ADC i obrazach z ważeniem T2. Skala Tonami dla pozytywnej sialografii MRI posłużyła jako punkt odniesienia do porównywania danych pochodzących z analizy tekstury. Wykazano, że wyższe oceny sialografii korelowały ze zwiększonymi wartościami ADC, co sugeruje, że ADC, często używane jako marker procesu zapalnego, może pomóc w szybkiej diagnozie wczesnego stadium SS (stopień 1). Zanotowano niższe wartości kurtozy i skośności w najwyższym stopniu skali Tonami, co prawdopodobnie wskazuje na zwiększoną heterogeniczność tkanki z powodu zaniku, rozrostu tkanki włóknistej i wypełnienia płynem sialectasis.

Głównym wnioskiem jest to, że parametry teksturalne stanowią obiecujące narzędzie do oceny zapalenia gruczołów ślinowych i mogą potencjalnie odgrywać rolę we wczesnej diagnozie i monitorowaniu zespołu Sjögrena. Złożona natura zespołu Sjögrena, jego zróżnicowane prezentacje kliniczne oraz ograniczenia tradycyjnych metod diagnostycznych powodują, że konieczne jest poszukiwanie innowacyjnych rozwiązań, takich jak analiza tekstury MRI. Badanie to wyróżnia kilka obszarów, w których analiza tekstury może poprawić proces diagnostyczny, takich jak wczesna diagnoza zespołu Sjögrena (stopień 1), monitorowanie przebudowy gruczołów ślinowych w procesie zespołu Sjögrena, zmniejszanie narażenia na promieniowanie oraz umożliwianie bardziej indywidualnego planowania leczenia. Integracja analizy tekstury z sekwencjami sialografii i mapami ADC prezentuje nowatorskie podejście do diagnozowania SS we wczesnym stadium u dzieci i przyczynia się do poprawy monitorowania choroby. W badaniu wykorzystano obrazowanie MRI do diagnozowania zespołu Sjögrena, charakteryzującego się nawracającym lub utrzymującym się powiększeniem gruczołów ślinowych u dzieci.

5. WNIOSKI

W pracy badawczej skupiono się na eksploracji i potwierdzeniu skuteczności analizy teksturalnej (TA) jako narzędzia wspomagającego w diagnostyce i monitoringu stanu zdrowia przy użyciu Obrazowania Rezonansem Magnetycznym (MRI).

W pierwszej pracy przedstawiono zastosowanie TA w monitorowaniu funkcji przeszczepionych nerek. Badania wykazały istotną korelację między parametrami teksturalnymi obrazów MRI a wskaźnikami funkcji nerek, co sugeruje potencjał TA w nieinwazyjnym monitorowaniu zdrowia i funkcji przeszczepionych nerek. Zaobserwowano, że cechy teksturalne regionu korowego nerki lepiej opisują funkcję nerki niż te z regionu piramid, co podkreśla znaczenie precyzyjnego umiejscowienia regionu zainteresowania (ROI) w TA.

W drugiej pracy skoncentrowano się na potencjale TA w diagnostyce zespołu Sjögrena u dzieci, gdzie wykorzystanie obrazowania MRI jest obiecującą metodą mogącą ulepszyć proces diagnostyczny. Badanie objęło analizę cech tekstury ekstrahowanych z obrazów MRI, co umożliwiło skuteczną identyfikację zmian strukturalnych gruczołów ślinowych. Wyniki wykazały korelację między cechami tekstury a stopniami morfologii MRI, co sugeruje możliwość wykorzystania TA jako narzędzia do wczesnej diagnozy zespołu Sjögrena oraz monitorowania przebudowy gruczołów ślinowych w procesie choroby.

Podsumowując, analiza teksturalna w diagnostyce obrazowej może znacząco poszerzyć możliwości diagnostyczne i terapeutyczne w medycynie. Umożliwienie lekarzom lepszego zrozumienia subtelnych zmian tkankowych może przełożyć się na lepsze wyniki leczenia i poprawę jakości życia pacjentów. Jednakże, wyniki obu prac podkreślają potrzebę dalszych badań w celu dokładnego zrozumienia możliwości, ograniczeń i praktycznego zastosowania TA w medycynie klinicznej.

SUMMARY IN ENGLISH

1. LIST OF ABBREVIATIONS

BMI	Body Mass Index
CKD	Chronic Kidney Disease
eGFR	Estimated Glomerular Filtration Rate
MDRD	Modification of Diet in Renal Disease
CKD	Chronic Kidney Disease Epidemiology Collaboration
TSE	Turbo Spin Echo
SPAIR	Spectral Presaturation with Inversion Recovery
3D TSE SPIR imaging	3D Turbo Spin Echo Spectral Presaturation with Inversion Recovery imaging
mDixon	Time consuming acquisition of in phase and opposed phase gradient echo images
STIR	Short TI Inversion Recovery
T2	The time constant for decay/dephasing of transverse magnetization
DWI	Diffusion weighted Imaging
ADC	Apparent Diffusion Coefficient
ROI	Region of Interest
FSO	First order statistic
GLCM	Gray Level Cooccurrence Matrix
GLSZM	Gray Level Size Zone Matrix
GLRLM	Gray Level Run Length Matrix
NGTDM	Neighboring Gray Tone Difference Matrix
GLDM	Gray Level Dependence Matrix
SAE	Small Area Emphasis
LAE	Large Area Emphasis
GLN	Gray Level Non-Uniformity
GLNN	Gray Level Non-Uniformity Normalized
SZN	Size Zone Non-Uniformity
SZNN	Size Zone Non-Uniformity Normalized
ZP	Zone Percentage
GLV	Gray Level Variance
ZV	Zone Variance
ZE	Zone Entropy
LGLZE	Low Gray Level Zone Emphasis
HGLZE	High Gray Level Zone Emphasis
SALGLE	Small Area Low Gray Level Emphasis
SAHGLE	Small Area High Gray Level Emphasis
LALGLE	Large Area Low Gray Level Emphasis
LAHGLE	Large Area High Gray Level Emphasis
SRE	Short Run Emphasis
LRE	Long Run Emphasis
RLN	Run Length Non-Uniformity
RLNN	Run Length Non-Uniformity Normalized
RP	Run Percentage
RV	Run Variance
RE	Run Entropy
LGLRE	Low Gray Level Run Emphasis
HGLRE	High Gray Level Run Emphasis
SRLGLE	Short Run Low Gray Level Emphasis
SRHGLE	Short Run High Gray Level Emphasis

LRLGLE	Long Run Low Gray Level Emphasis
LRHGLE	Long Run High Gray Level Emphasis
SDE	Small Dependence Emphasis
LDE	Large Dependence Emphasis
DN	Dependence Non-Uniformity
DNN	Dependence Non-Uniformity Normalized
DV	Dependence Variance
DE	Dependence Entropy
LGLE	Low Gray Level Emphasis
HGLE	High Gray Level Emphasis
SDLGLE	Small Dependence Low Gray Level Emphasis
SDHGLE	Small Dependence High Gray Level Emphasis
LDLGLE	Large Dependence Low Gray Level Emphasis
LDHGLE	Large Dependence High Gray Level Emphasis

2. INTRODUCTION

Texture analysis, applied in medical imaging, particularly in magnetic resonance imaging (MRI), is an innovative technique that can change how doctors perceive and interpret medical images. By utilizing advanced algorithms to analyze texture details, this method allows the extraction of more information from images, providing doctors with a deeper understanding of tissue structures and microstructures. This subtle analysis goes beyond the capabilities of traditional imaging techniques, enabling the detection of molecular and tissue-level changes that may be crucial for early recognition, monitoring, and treatment of various disease entities.

The texture of an MRI image, understood as a complex pattern of voxel intensities, can reveal significant information about tissue composition, structure, and function. Texture analysis uses parameters such as contrast, uniformity, or entropy, among others, to assess and interpret these patterns, allowing for the identification of subtle differences in tissue images, often invisible to standard imaging diagnostic methods. Thus, texture analysis opens new perspectives in medical diagnostics, offering a tool capable of potentially early disease detection, precise therapy progress monitoring, and adjusting treatment to individual patient needs.

Texture analysis can become an invaluable tool in oncology, where early detection and monitoring of therapy response are crucial. It may allow the identification of microscopic changes in tumor tissue, which may indicate a response to treatment or lack thereof, even before any changes in tumor size are visible to the eye of radiologists. This, in turn, may enable doctors to quickly modify the treatment plan, thereby increasing the patient's chances of recovery.

Moreover, texture analysis can play a key role in personalized medicine. By identifying unique textural patterns associated with specific pathological conditions, doctors may be able to modify therapy to the individual characteristics of a patient's disease, which can significantly improve treatment effectiveness. The personalization of therapy, based on precise diagnosis, thus becomes more reasonable, marking a significant advancement in medicine and contributing to an increase in the chances of therapeutic success.

Patient safety and comfort are other important aspects that texture analysis can significantly impact. As a non-invasive method using images that patients routinely obtain during diagnostics, it can significantly reduce the risk of complications associated with invasive diagnostic procedures. This may make it particularly valuable in cases where frequent patient condition monitoring is necessary, such as in chronic diseases or oncology. Moreover, the non-invasive nature of texture analysis may make it a safe and patient-friendly method, including for children and high-risk groups.

Another example may be the importance of this method in neurology, where texture analysis can also play a crucial role, enabling a better understanding of the mechanisms of neurodegenerative diseases. Through the analysis of subtle changes in brain structure, doctors may be better able to understand how diseases such as Alzheimer's or multiple sclerosis affect brain tissue, which may lead to earlier diagnosis and better therapy adjustment.

In conclusion, texture analysis in medical imaging is a technological breakthrough that can significantly expand diagnostic and therapeutic possibilities in medicine. It offers the possibility of early disease detection and precise treatment monitoring and may pave the way for more personalized and effective medical care. By enabling doctors to understand subtle tissue changes more deeply, texture analysis can contribute to faster and more informed clinical decision-making, which may translate into better treatment outcomes and improved quality of

life for patients. In an era where precision and personalization in medicine are increasingly sought after, texture analysis stands out as a key tool supporting the development of modern, patient-centered healthcare.

3. AIMS OF THE STUDY

The primary objective of the research was to explore and validate Textural Analysis (TA) as a supplementary tool in diagnostics and health status monitoring using Magnetic Resonance Imaging (MRI). Specifically, these studies aimed to refine and confirm TA as a complementary method to existing diagnostic approaches, enhancing the accuracy of diagnosing and monitoring patients' health, thereby increasing the precision and efficiency of diagnostics.

1. First Article:

   Objective: To assess the potential role of TA in monitoring the function of transplanted kidneys.
   Specific Objective: To present TA as a method enabling the identification of correlations between texture parameters and kidney function indicators (such as eGFR and creatinine).

2. Second Article:

   Objective: To investigate the possibilities of using TA in assessing the salivary glands' condition in the context of Sjögren's syndrome in children.
   Specific Objective: To demonstrate that TA can serve as a tool for non-invasive and potential differentiation of pathological conditions of the salivary glands, which can be particularly valuable in the diagnostic challenges associated with Sjögren's syndrome.

In summary, the overriding goal is to develop and confirm the effectiveness of TA as a tool complementing standard MRI methods, hoping to improve diagnostics and health status monitoring without additional invasive procedures. Both articles emphasize the need for further research to fully understand TA's capabilities, limitations, and practical application in clinical medicine. They point to the potential of TA as a tool complementing standard MRI methods, with the hope of enhancing diagnostic and health monitoring processes, while noting that further research is necessary to exploit the possibilities of TA fully.

4. DESCRIPTION OF THE PUBLICATIONS INCLUDED IN THE DOCTORAL THESIS

1. Publication 1.

Computation of the texture features on T2-weighted images as a novel method to assess the function of the transplanted kidney: primary research.

The study represents an innovative exploration of using textural analysis (TA) to evaluate renal function after kidney transplantation (KTx). The research is predicated on the hypothesis that TA, applied to T2-weighted MRI images, could effectively assess renal function in patients who have undergone a kidney transplant. The study particularly analyzes the texture features of T2-weighted images from nine patients with transplanted kidneys, aiming to discern a statistical difference in these features based on the placement of the region of interest (ROI) within the kidney.

The research methodology retrospective examinations of MRI scans from the selected patients. The focus on T2-weighted images is particularly pertinent, given their relevance in renal imaging. The study is based on measures the texture features and correlates these features with the estimated glomerular filtration rate (eGFR) calculated using the Chronic Kidney Disease Epidemiology Collaboration (CKD-EPI) formula. Statistical analyses, including the Spearman correlation test and the Mann-Whitney U test, are utilized to ensure the validity of the findings.

The results of the study are promising. A significant correlation is observed between the texture parameters of the T2-weighted images and the renal function indicators, mainly eGFR and creatinine levels. This correlation is particularly pronounced when the ROI is positioned within the kidney cortex, suggesting that the cortical region's texture features are more indicative of renal function than those of the medullary region. The study also discovers significant differences in texture parameters based on the placement of ROI, affirming the hypothesis that the spatial distribution of ROI within the kidney influences the texture analysis results.

The article delves deeper into the implications of these findings. The significant correlation between certain texture parameters and renal function indicators, particularly within the cortical region, underscores the potential of TA in non-invasively monitoring the health and function of transplanted kidneys. The lack of a significant correlation between texture features and renal function indicators when considering the whole kidney ROI is an intriguing finding, emphasizing the complexity of renal structure and function and the need for precise ROI placement in TA.

The textural analysis of T2-weighted MRI images can be a good tool for assessing the function of transplanted kidneys. The significant correlations observed between texture parameters and key indicators of renal function, particularly in the kidney cortex, offer a new avenue for non-invasive, imaging-based monitoring of kidney transplant recipients. However, the research also acknowledges the need for further studies, especially to determine the optimal binning of ROI size and its placement within the organ to harness the potential of TA in this context fully.

In summary, this pioneering research presents a compelling case for using textural analysis of T2-weighted MRI images to assess the function of transplanted kidneys. The observed correlation between texture parameters and renal function indicators opens up new possibilities

for the non-invasive monitoring of kidney transplants. Nevertheless, the study also points towards the need for more comprehensive research to refine the methodology and fully realize the potential of this innovative approach.

2. Publication 2.

Textural analysis of magnetic resonance images as an additional evaluation tool of parotid glands in Sjögren - primarily findings

Sjögren's Syndrome (SS) in pediatric patients presents unique diagnostic challenges due to its nonspecific and often delayed clinical presentation. Traditional diagnostic methods, including salivary gland ultrasound, sialography, and scintigraphy, offer valuable insights but have significant limitations and risks. MRI sialography is underutilized, and texture analysis of MRI images is emerging as a promising method to improve the diagnostic process.

This study included 36 patients with a positive small labial salivary gland biopsy for SS and a control group of 20 children or young adolescents. The examination protocol encompassed a survey sequence and morphological sequences in three planes. The primary sequences were diffusion-weighted imaging (DWI) and T2-weighted imaging, facilitating a comprehensive evaluation of the anatomical and pathological aspects of the patients and playing a fundamental role in understanding Sjögren's Syndrome in the pediatric population.

The study utilized magnetic resonance imaging (MRI) to assess the state of salivary glands based on the Tonami-modified criteria. The high T2 signal intensity size across all areas of the glands in the MRI sialography sequence determined the evaluation. The N4 algorithm was employed to correct field inhomogeneity, thus enhancing the quality and accuracy of the analysis. The region of interest (ROI) was manually delineated to encompass all glands, with a margin of 1 mm from the edge, to minimize potential influences from surrounding tissues or artifacts.

The texture features extracted from these ROIs were categorized into subgroups: First Order Statistics, Gray Level Co-occurrence Matrix, Gray Level Size Zone Matrix, Gray Level Run Length Matrix, Neighboring Gray Tone Difference Matrix, and Gray Level Dependence Matrix. Statistical analyses were conducted using SPSS Statistics 27. The Shapiro-Wilk test revealed that the parameters did not follow a normal distribution, prompting the use of the Spearman correlation test to explore the relationships between the collected data and identify correlations between texture features in diseased and healthy glands. The Independent-Samples Kruskal-Wallis Test was applied to compare group differences among the glands, and post hoc analysis was conducted to pinpoint significant differences between groups, with a significance level set at $p<0.05$.

The study evaluated the MRI sialography grades for each gland, considering the presence of cystic changes. The observed distribution was Grade 0 in 12 glands (16%), Grade 1 in 8 glands (11%), Grade 2 in 30 glands (42%), and Grade 3 in 22 glands (31%). The mean Apparent Diffusion Coefficient (ADC) value for SS patients and the control group was derived from the ROI in each gland, with the mean ADC value being contingent on the MRI morphology grade. Statistically significant differences ($p<0.05$) were noted between groups: 1 - healthy ($p= 0.005$), 1-3 ($p=0.046$), 0 - 3 ($p=0.035$), and 0 - healthy ($p=0.001$). Whole-volume ADC images for texture analysis were generated for each gland, without differentiation between the left and right glands. A moderate correlation was found between texture features and MRI morphology grades, and a positive and moderate correlation was specifically noted between individual MRI

morphology parameters and certain texture parameters, particularly the First Order Statistics parameters. This correlation suggests that the First Order Statistics parameters can effectively delineate crucial details about the structural features of the gland as visualized in the MRI images.

The study also compared the mean values of image and texture analysis of ADC images to MRI Tonami grades. The parameters included Tonami Scale, entropy, kurtosis, skewness, GLDM_Dependence NonUniformity, GLDM_Small Dependence High Gray Level Emphasis, GLCM_Imc1, GLRLM_Run Entropy, and GLSZM_Zone Entropy. The results indicated that the ADC values corresponded closely with MRI Tonami grades, evidenced by a mean of 0.01, a standard deviation of 0.00, and a kurtosis of 3.86. Moreover, GLDM_Dependence NonUniformity and GLDM_Small Dependence High Gray Level Emphasis demonstrated similar values, suggesting the potential of ADC images for MRI Tonami analysis.

The study explored the texture of salivary glands in MRI images within a pediatric cohort of Sjogren syndrome patients. It examined the textural differences within two regularly acquired MRI sequences in SS patients - ADC maps and T2-weighted images. The Tonami scale for positive MRI sialography was the benchmark for comparing data derived from texture analysis. The findings showed that higher sialography grades were associated with increased ADC values, implying that ADC, commonly used as an inflammatory marker, can aid in promptly diagnosing early-stage SS (grade 1). Lower kurtosis and skewness values were noted in the highest Tonami Scale grade, likely indicative of increased tissue heterogeneity due to atrophy, fibrotic tissue replacement, and fluid-filled sialectasis.

The textural parameters are a promising tool for assessing parotid gland inflammation and could potentially play a role in the early diagnosis and monitoring of Sjögren's Syndrome. The complex nature of Sjögren's Syndrome, its varied clinical presentations, and the limitations of traditional diagnostic methods underscore the importance of exploring innovative approaches like texture analysis of MRI. This study highlights several areas where texture analysis can enhance the diagnostic process, such as early diagnosis of Sjögren's Syndrome (grade 1), monitoring salivary gland remodeling in Sjögren's Syndrome, reducing radiation exposure, and facilitating more individualized treatment planning. The integration of texture analysis with sialography sequences and ADC maps presents a novel approach to the early-stage diagnosis of SS in children and contributes to improved disease monitoring. This study uses MRI imaging to diagnose Sjögren's Syndrome, characterized by recurrent or persistent salivary gland enlargement in children.

5. SUMMARY

The research focused on exploring and confirming the effectiveness of texture analysis (TA) as a supporting tool in diagnostics and monitoring health status using Magnetic Resonance Imaging (MRI).

In the first study, the application of TA in monitoring the function of transplanted kidneys was presented. Research showed a significant correlation between the textural parameters of MRI images and kidney function indicators, suggesting the potential of TA in non-invasive monitoring of health and function of transplanted kidneys. It was observed that the textural features of the cortical region of the kidney better describe kidney function than those from the pyramid region, emphasizing the importance of the precise placement of the region of interest (ROI) in TA.

In the second study, the focus was on the potential of TA in diagnosing Sjögren's syndrome in children, where the use of MRI imaging is a promising method that could improve the diagnostic process. The study involved analyzing the texture features extracted from MRI images, which effectively identified structural changes in the salivary glands. The results showed a correlation between texture features and MRI morphology degrees, suggesting the possibility of using TA as a tool for early diagnosis of Sjögren's syndrome and monitoring the remodeling of salivary glands in the disease process.

In summary, texture analysis in imaging diagnostics can significantly expand medical diagnostic and therapeutic possibilities. By enabling doctors to understand subtle tissue changes, it can lead to better treatment outcomes and improve patients' quality of life. However, the results of both studies emphasize the need for further research to fully understand the possibilities, limitations, and practical application of TA in clinical medicine.

BIBLIOGRAFIA / REFERENCES

1. Stefanski, A.-L.; Tomiak, C.; Pleyer, U.; Dietrich, T.; Burmester, G.R.; Dörner, T. The Diagnosis and Treatment of Sjögren's Syndrome. *Dtsch. Ärzteblatt Int.* **2017**, *114*, 354.
2. Shiboski, C.H.; Shiboski, S.C.; Seror, R.; Criswell, L.A.; Labetoulle, M.; Lietman, T.M.; Rasmussen, A.; Scofield, H.; Vitali, C.; Bowman, S.J.; et al. 2016 American College of Rheumatology/European League Against Rheumatism Classification Criteria for Primary Sjögren's Syndrome: A Consensus and Data-Driven Methodology Involving Three International Patient Cohorts. *Arthritis. Rheumatol.* **2017**, *69*, 35–45.
3. Jonsson, M.V.; Baldini, C. Major Salivary Gland Ultrasonography in the Diagnosis of Sjögren's Syndrome: A Place in the Diagnostic Criteria? *Rheum. Dis. Clin. N. Am.* **2016**, *42*, 501–517.
4. Pomorska, A.; Świętoń, D.; Lieberman, S.M.; Bryl, E.; Kosiak, W.; Pęksa, R.; Chorąży ewicz, J.; Kochańska, B.; Kowalska-Skabara, J.;Szumera, M.; et al. Recurrent or persistent salivary gland enlargement in children: When is it Sjögren's? *Semin. Arthritis Rheum.***2022**, *52*, 151945.
5. Świecka, M.; Maślińska, M.; Paluch, Ł.; Zakrzewski, J.; Kwiatkowska, B. Imaging methods in primary Sjögren's Syndrome as potential tools of disease diagnostics and monitoring. *Reumatologia/Rheumatology* **2019**, *57*, 336–342
6. Buus, S.; Grau, C.; Munk, O.L.; Bender, D.; Jensen, K.; Keiding, S. 11C-methionine PET, a novel method for measuring regional salivary gland function after radiotherapy of head and neck cancer. *Radiother. Oncol.* **2004**, *73*, 289–296.
7. Takashima, S.; Takeuchi, N.; Morimoto, S.; Tomiyama, N.; Ikezoe, J.; Shogen, K.; Kozuka, T.; Okumura, T. MR Imaging of Sjögren Syndrome. *J. Comput. Assist. Tomogr.* **1991**, *15*, 393–400.
8. Chu, C.; Feng, Q.; Zhang, H.; Zhu, Y.; Chen, W.; He, J.; Sun, L.; Zhou, Z. Whole-Volume ADC Histogram Analysis in Parotid Glands to Identify Patients with Sjögren's Syndrome. *Sci. Rep.* **2019**, *9*, 9614.
9. Chu, C.; Wang, F.; Zhang, H.; Zhu, Y.; Wang, C.; Chen, W.; He, J.; Sun, L.; Zhou, Z. Whole-volume ADC Histogram and Texture Analyses of Parotid Glands as an Image Biomarker in Evaluating Disease Activity of Primary Sjögren's Syndrome. *Sci. Rep.* **2018**, *8*, 15387.
10. Ganeshan, B.; Skogen, K.; Pressney, I.; Coutroubis, D.; Miles, K. Tumour heterogeneity in oesophageal cancer assessed by CT texture analysis: Preliminary evidence of an association with tumour metabolism, stage, and survival. *Clin. Radiol.* **2012**, *67*, 157–164.
11. Chen, P.; Dong, B.; Zhang, C.; Tao, X.; Wang, P.; Zhu, L. The histogram analysis of apparent diffusion coefficient in differential diagnosis of parotid tumor. *Dentomaxillofacial. Radiol.* **2020**, *49*, 20190420.
12. Tonami, H.; Higashi, K.; Matoba, M.; Yokota, H.; Yamamoto, I.; Sugai, S. A Comparative Study Between MR Sialography and Salivary Gland Scintigraphy in the Diagnosis of Sjögren Syndrome. *J. Comput. Assist. Tomogr.* **2001**, *25*, 262–268.
13. Tustison, N.J.; Avants, B.B.; Cook, P.A.; Zheng, Y.; Egan, A.; Yushkevich, P.A.; Gee, J.C. N4ITK: Improved N3 bias correction. *IEEE Trans. Med. Imaging* **2010**, *29*, 1310e20
14. Pyradiomics Organization. Pyradiomics Documentation. 2019. Available online: https://pyradiomics.readthedocs.io/en/latest/ (accessed on 1 April 2023).
15. Castellano, G.; Bonilha, L.; Li, L.M.; Cendes, F. Texture analysis of medical images. *Clin. Radiol.* **2004**, *59*, 1061e9.
16. Kalk, W.W.; Vissink, A.; Spijkervet, F.K.; Bootsma, H.; Kallenberg, C.G.; Roodenburg, J.L. Parotid sialography for diagnosing Sjögren syndrome. *Oral Surg. Oral Med. Oral Pathol. Oral Radiol. Endod.* **2002**, *94*, 131–137.]
17. Ng, F.; Ganeshan, B.; Kozarski, R.; Miles, K.A.; Goh, V. Assessment of primary colorectal cancer heterogeneity by using whole-tumor texture analysis: Contrast-enhanced CT texture as a biomarker of 5-year survival. *Radiology* **2013**, *266*, 177–184
18. Márton, K.; Boros, I.; Fejérdy, P.; Madléna, M. Evaluation of unstimulated flow rates of whole and palatal saliva in healthy patients wearing complete dentures and in patients with Sjogren's Syndrome. *J. Prosthet. Dent.* **2004**, *91*, 577–581.
19. Tzioufas, A.G.; Moutsopoulos, H.M. Salivary gland imaging techniques for the diagnosis of Sjögren's Syndrome. *Int. J. Clin. Rheumtol.* **2009**, *4*, 321–327
20. Makanyanga, J.; Ganeshan, B.; Rodriguez-Justo, M.; Bhatnagar, G.; Groves, A.; Halligan, S.; Miles, K.; Taylor, S.A. MRI texture analysis (MRTA) of T2-weighted images in Crohn's disease may provide information on histological and MRI disease activity in patients undergoing ileal resection. *Eur. Radiol.* **2017**, *27*, 589
21. de Figueiredo, E.H.; Borgonovi, A.F.; Doring, T.M. Basic Concepts of MR Imaging, Diffusion MR Imaging, and Diffusion Tensor Imaging. Magn. Reason. *Imaging Clin. N. Am.* **2011**, *19*, 1–22.
22. Cohen, J.; Cohen, P.; West, S.G.; Aiken, L.S. *Applied Multiple Regression/Correlation Analysis for the Behavioral Sciences*, 3rd ed.; Lawrence Erlbaum Associates, Inc.: Mahwah, NJ, USA, 2003.
23. Cho, S.H.; Kim, G.C.; Jang, Y.-J.; Ryeom, H.; Kim, H.J.; Shin, K.-M.; Park, J.S.; Choi, G.-S.; Kim, S.H.

Locally advanced rectal cancer: Post-chemoradiotherapy ADC histogram analysis for predicting a complete response. *Acta Radiol.* **2015**, *56*, 1042–1050.
24. Zhong, W.; Zhang, H.; Ran, H. Advances in imaging of the lacrimal gland in Sjögren's Syndrome: A narrative review. *J. Clin. Ultrasound* **2023**, 1–10
25. Muntean, D.D.; Bădărînză, M.; S, tefan, P.A.; Lenghel, M.L.; Rusu, G.M.; Csutak, C.; Coroian, P.A.; Lupean, R.A.; Fodor, D. The Diagnostic Value of MRI-Based Radiomic Analysis of Lacrimal Glands in Patients with Sjögren's Syndrome. *Int. J. Mol. Sci.* **2022**, *23*, 10051.
26. Freni, F.; Gazia, F.; D'alcontres, F.S.; Galletti, B.; Galletti, F. Use of botulinum toxin in Frey's syndrome. *Clin. Case Rep.* **2019**, *7*, 482–485.
27. Furness, S.; Bryan, G.; McMillan, R.; Worthington, H.V. Interventions for the Management of Dry Mouth: Non-Pharmacological Interventions. In *Cochrane Database of Systematic Reviews*; Furness, S., Ed.; John Wiley & Sons, Ltd.: Chichester, UK, 2013.
28. Hammenfors, D.S.; Valim, V.; Bica, B.E.R.G.; Pasoto, S.G.; Lilleby, V.; Nieto-González, J.C.; Silva, C.A.; Mossel, E.; Pereira, R.M.R.; Coelho, A.; et al. Juvenile Sjögren's Syndrome: Clinical Characteristics with Focus on Salivary Gland Ultrasonography. *Arthritis. Care Res.* **2020**, *72*, 78–87
29. Abbasian Ardakani A, Mohammadi A, Khalili Najafabad B, Abolghasemi J. Assessment of kidney function after allograft transplantation by texture analysis. Iran J Kidney Dis 2017;11: 157e64.
30. Kee TYS, Chapman JR, O'Connell PJ, Fung CLS, Allen RDM, Kable K, et al. Treatment of subclinical rejection diagnosed by protocol biopsy of kidney transplants. Transplantation 2006;82:36e42. https://doi.org/10.1097/01.tp.0000225783.86950.c2.
31. Materka A. Texture analysis methodologies for magnetic resonance imaging. Dialogues Clin Neurosci 2004;6:243e50.
32. Castellano G, Bonilha L, Li LM, Cendes F. Texture analysis of medical images. Clin Radiol 2004;59:1061e9. https://doi.org/10. 1016/j.crad.2004.07.008.
33. Tustison NJ, Avants BB, Cook PA, Zheng Y, Egan A, Yushkevich PA, et al. N4ITK: improved N3 bias correction. IEEE Trans Med Imaging 2010;29:1310e20. https://doi.org/10.1109/TMI. 2010.2046908.
34. van Griethuysen JJM, et al. Computational radiomics system to decode the radiographic phenotype. American Association for Cancer Research 2017;77(21). https://doi.org/10.1158/0008-5472. CAN-17-0339.
35. Kickingereder P, Burth S, Wick A, Götz M, Eidel O, Schlemmer HP, et al. Radiomic profiling of glioblastoma: identifying an imaging predictor of patient survival with improved performance over established clinical and radiologic risk models. Radiology 2016;280:880e9. https://doi.org/10.1148/radiol.2016160845.
36. de Leon AD, Kapur P, Pedrosa I. Radiomics in kidney cancer: MR imaging. Magn Reson Imaging Clin N Am 2019;27: 1e13. https://doi.org/10.1016/j.mric.2018.08.005.
37. Nioche C, Orlhac F, Boughdad S, Ruezé S, Goya-Outi J, Robert C, et al. LIFEX: a freeware for radiomic feature calculation in multimodality imaging to accelerate advances in the character- ization of tumor heterogeneity. Cancer Res 2018;78:4786e9. https:// doi.org/10.1158/0008-5472.CAN-18-0125.

PUBLIKACJE WCHODZĄCE W SKŁAD ROZPRAWY DOKTORSKIEJ / MANUSCRIPTS INCLUDED IN THE DOCTORAL DISSERTATION

Computation of the Texture Features on T2-Weighted Images as a Novel Method to Assess the Function of the Transplanted Kidney: Primary Research

Małgorzata Grzywinska[a,*], Magdalena Jankowska[b], Ewa Banach-Ambroziak[c], Edyta Szurowska[c], and Alicja Dębska-Slizień[b]

[a]Department of Human Physiology, Medical University of Gdansk, Gdansk, Poland;

[b]Department of Nephrology, Transplantology and Internal Medicine, Medical University of Gdansk, Gdansk, Poland; and

[c]Second Department of Radiology, Medical University of Gdansk, Gdansk, Poland

ABSTRACT

Texture in medical images describes the internal structure of human tissues or organs. We hypothesize that textural analysis (TA) could be applied to assess renal function after kidney transplantation (KTx). This preliminary study aims to find a statistical difference between texture features in transplanted kidneys with different placement of region of interest (ROI). Also, we aimed at comparing results of TA with transplanted kidney function. For analysis, we used 9 retrospective examinations in patients with a transplanted kidney. All patients underwent a diagnostic magnetic resonance imaging (MRI) scan, including T2-weighted images. All MRI acquisition was performed using a 1.5T MRI (MAGNETOM Aera, Siemens Healthineers AG, Erlangen, Germany). Examinations were performed from indications other than KTx and in various times after KTx. We found an association between the texture parameters and the estimated glomerular filtration rate (4p estimate formula: Chronic Kidney Disease Epidemiology Collaboration [CKD-EPI]) and between texture parameters and creatinine in ROI location in the cortex. Our findings make TA a promising tool for the assessment of the function of the transplanted kidney. However, the effect of binning, ROI size, and placement of ROI in the organ are yet to be determined and need further study.

levels. Ultrasonography, computed tomography (CT), nuclear medicine, or magnetic resonance imaging (MRI) are also used to evaluate kidneys. Both ultrasonography and MRI have an advantage over other modalities because of the lack of ionizing radiation [1]. Ultrasonography is easily accessible, and the kidney condition can be evaluated in real time. MRI is a rapidly developing imaging technique that improves the quality of organ evaluation; therefore, more often, it is used as the second choice after ultrasonography.

One of the promising and constantly developing methods of the organ function evaluation is imaging the texture of kidneys in the MRI study. The texture in the radiological sense is described as the micro- and macro-structure of the selected area or element of the organ. The texture is perceived as a visualization of complex, spatially arranged the image are perceived to exhibit specific brightness, color, roughness, directionality, randomness, smoothness, grain, uniformity, and density. The texture may contain relevant information about the structure of physical objects [3e5]. In medical images, it shows the internal structure of human tissues or organs. Although textures are readily perceivable by people, there is no strict definition of what constitutes texture regarding image processing. Textural analysis and the measurement of conventional parameters from imaging

*Address correspondence to Małgorzata Grzywinska, Medical University of Gdansk, Department of Human Physiology, Tuwima 15, 80-210, Gdansk, Poland. Tel: þ48 58 349 15 15. E-mail: malgorzata.grzywinska@gumed.edu.pl

0041-1345/20
https://doi.org/10.1016/j.transproceed.2020.02.084

THE most commonly used method for monitoring kidney patterns and repeating subsuppliers that have a charactertransplant function is to monitor serum creatinine istic, slightly uniform appearance [2]. Local subdivisions in

Table 1. Demographic Information

No.	Age	Sex	Original Disease	BMI	eGFR MDRD (mL/min/1.73 m)	eGFR CKD (mL/min/1.73 m)	Creatinine (mg/dL)	Proteinuria	Time post-transplant (y)	Donor Source (Live/ Deceased Donor)
1	32	Female	Renal amyloidosis secondary to familial Mediterranean fever	25.78	>60.0	>90	0.63	-	16	Deceased donor
2	65	Female	Glomerulonephritis	15.15	>60.0	>90	0.64	-	7	Deceased donor
3	43	Female	Chronic renal failure of unknown origin, most likely chronic pyelonephritis	21.88	>60.0	>90	0.75	-	2	Deceased donor
4	60	Male	Glomerulonephritis	24.58	33.1	36	1.98	Trace	18	Deceased donor
5	59	Male	Chronic renal failure of unknown origin, probably hypertensive nephropathy	27.78	35.0	37	1.95	-	13	Deceased donor
6	37	Female	Chronic glomerulonephritis in the course of postinflammatory/ noninfective nephropathy	22.89	33.0	37	1.73	-	2	Deceased donor
7	48	Female	Chronic kidney disease	15.39	59.0	66	1.01	-	4	Deceased donor
8	44	Female	Renal failure in the course of diabetic nephropathy	29.76	49.0	55	1.20	-	19	Deceased donor
9	45	Male	Renal failure	27.78	>60.0	68	1.27	-	8	Deceased donor

Abbreviations: BMI, body mass index; CKD, chronic kidney disease; eGFR, estimated glomerular filtration fate; MDRD, Modification of Diet in Renal Disease.

studies is based on a series of algorithms related to the series of images [6].

The main aim of the study was to demonstrate the usefulness of textural analysis of MRI for the analysis of transplanted kidney function.

MATERIAL AND METHODS

For analysis, we used retrospective examinations in 9 patients with a transplanted kidney. All patients underwent a diagnostic MRI scan, including T2-weighted images [7]. All MRI acquisition was performed using a 1.5T MRI (Magnetom Aera, Siemens Healthineers, Germany). The examination was performed within different times after transplantation (2-19 years) and from various indications (Table 1).

We used the N4 algorithm to correct the field inhomogeneity [8]. Then, we used Pyradiomics (v2.0.0) [9] for texture analysis, an absolute bound, and bin width fixed. ROI was drawn in the cortex and all over the kidney (Fig 1) [10].

The kidney function was assessed as estimated glomerular filtration fate (eGFR) calculation (4p estimate formula: Chronic Kidney Disease Epidemiology Collaboration [CKD-EPI]) (min: 37; max: >90 mL/min/1.73 m^2) on the day of the MRI examination.

Statistical analysis was performed using SPSS Statistics 25 (IBM, Armonk, NY, United States). All results were tested for normal distribution with the Shapiro-Wilk test for each protocol. Because this test has shown a non-normal distribution, we used the Spearman correlation test to show the correlation between obtained data. The Mann-Whitney U test was used to analyze the difference between the features in various ROI.

RESULTS

We found an association between the texture parameters and eGFR, and texture parameters and creatinine in ROI location in the cortex. Tables 2 and 3 show parameters that were statistically significant in both eGFR formula and creatinine. We found no statistically significant correlation between eGFR and texture parameters and creatinine and parameters for a whole kidney ROI.

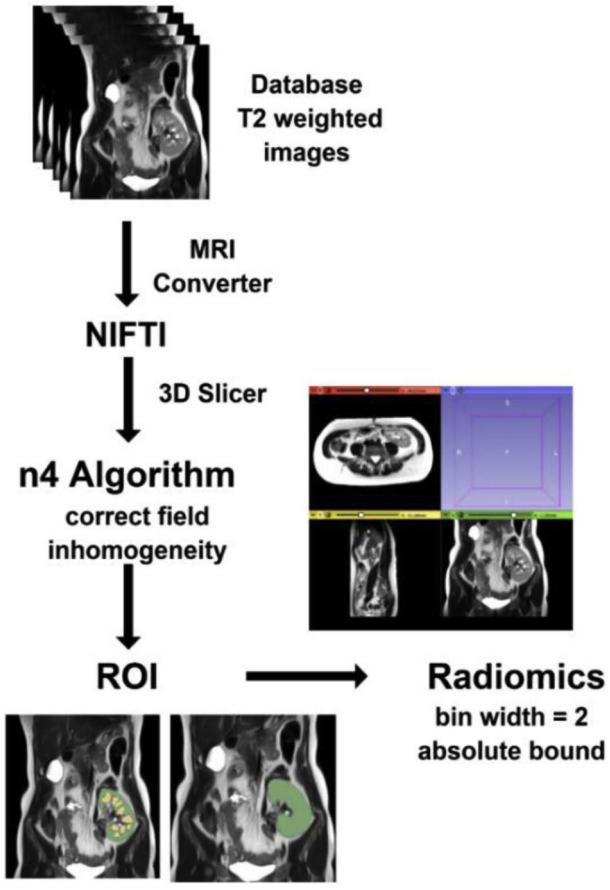

Fig 1. Procedure of analysis. MRI, magnetic resonance imaging.

Table 2. Relation Between the Texture Parameters and eGFR CKD in ROI Location in the Cortex

Features	Parameter	eGRF CKD-EPI R	eGRF CKD-EPI P Value
Gray level dependence matrix	High gray level emphasis	0.899	.015
	Small dependence high gray level emphasis	0.986	< .001
	Large dependence low gray level emphasis	-0.899	.015
Gray level co-occurrence matrix	Joint average	0.899	.015
	Sum average	0.899	.015
	Autocorrelation	0.899	.015
Gray level run length matrix	Short run high gray level emphasis	0.899	.015
	High gray level run emphasis	0.899	.015
Gray level size zone matrix	Small area high gray level emphasis	0.899	.015
	High gray level zone emphasis	0.899	.015
Neighboring gray tone difference matrix	Strength Busyness	0.812	.050
		-0.899	.015

Abbreviations: CKD-EPI, Chronic Kidney Disease Epidemiology Collaboration; eGFR, estimated glomerular filtration fate.

An additional finding was a significant difference between texture parameters with different placement of ROI (in all kidney and in the cortex). However, we did not find any significant difference between the texture features between ROI in cortex and pyramids (Table 4).

DISCUSSION

The results of our study showed a significant association between some texture parameters and creatinine or eGFR from ROI placed in the cortex (Tables 2 and 3). Concerning eGFR, we observed a strong association with the features in gray level dependence, gray level co-occurrence, gray level run length, gray level size zone, and neighboring gray tone difference matrix. However, no correlation was found between creatinine and eGFR and the whole kidney ROI. This finding might be easily explained by the fact that the cortex holding the glomeruli load reflects the filtration capacity to a higher extent than the medulla. Thus, whole kidney ROI should have much lesser impact in reflecting GFR.

Different methods of image analysis can be used to characterize the heterogeneity of the change. We used both approaches. The most commonly used methods are based on histogram analysis of voxel values in the area of interest and methods of the spatial distribution of voxel values. In histogram-based methods, the algorithms used to bypass the intrinsic spatial relationship between voxel values reflect only the frequency of the presence of voxels with the same signal intensity [5]. In this method, we obtained a moderate correlation between the texture parameters and creatinine in location ROI in the cortex.

The second approach of texture analysis considers the spatial distribution of voxel values in the organ using higher statistical values, first calculating the two-dimensional matrix describing this spatial organization. This matrix is often a gray coordinate matrix, which makes it possible to observe a pair of voxels at a given distance in a given direction. Several other matrices are also used, among which there is a gray neighborhood matrix, which provides information on how each value of the voxel differs from the voxel values of the neighbor. All matrices capture a specific spatial relationship between the values of voxels, and each matrix allows the calculation of several heterogeneity descriptors [3,11]. With this method, we found that both creatinine and eGFR are correlated with some texture features. On this basis, we may gain additional information about the function or heterogeneity of kidneys without additional examination.

Initial research, like ours, is being carried out on the correlation of textural parameters with the clinical data of patients. The published data on this highly novel approach are scarce. One of the reports concerned textural analysis in ultrasonography [12]. In this study, textural parameters such as co-occurrence matrix, runlength matrix, and histogram were also shown to associate with creatinine and eGFR, which aligns with our findings. Our findings support the previous suggestions that a change in the intensity of pixels may suggest

Table 3. Relation Between the Texture Parameters and Creatinine in Location Region of Interest in the Cortex

Features	Parameter	Creatinine R	Creatinine P Value
Gray level dependence matrix	Dependence nonuniformity	0.617	.039
	Gray level nonuniformity	0.600	.044
	Small dependence high gray level emphasis	-0.650	.029
Gray level co-occurrence matrix	Informational measure of correlation 2	-0.833	.003
	Informational measure of correlation 1	-0.917	< .001
	Cluster tendency	-0.600	.044
First order	Skewness	0.767	.008
	Median	-0.583	.049
	Root mean squared	-0.583	.049
	90th percentile	-0.583	.049
	10th percentile	-0.583	.049
	Mean	-0.583	.049
Gray level run length matrix	Gray level nonuniformity	0.600	.044
	Run length nonuniformity	0.633	.067
Gray level size zone matrix	Size zone nonuniformity	0.817	.004
	Gray level nonuniformity	0.700	.018

	Small area high gray level emphasis	-0.600	.044
Neighboring gray tone difference matrix	Coarseness	-0.867	.001
	Strength	-0.683	.042
	Busyness	0.733	.025

IMC, informational measure of correlation

T2-WEIGHTED IMAGES AND TRANSPLANTED KIDNEY FUNCTION

Table 4. Difference Between Texture Parameters With Different Placement of Region of Interest (in All Kidney and in the Cortex)

Features	Parameter	Z Score	P Value
Gray level dependence matrix	Gray level variance	-3.046	.002
	Dependence entropy	-3.311	.001
	Dependence nonuniformity	-3.311	.001
	Large dependence low gray level emphasis	-1.987	.047
	Small dependence low gray level emphasis	-3.311	.001
	Low gray level emphasis	-3.311	.001
Gray level cooccurrence matrix	Joint entropy	-3.311	.001
	Cluster shade	-3.400	.001
	Maximum probability	-3.135	.002
	Joint energy	-3.223	.001
	Contrast	-2.782	.005
	Difference entropy	-2.428	.015
	Inverse variance	-2.163	.031
	Difference Variance	-2.782	.005
	Inverse difference moment	-2.163	.031
First order	Interquartile range	-2.782	.005
	Skewness	-1.987	.047
	Energy	-3.488	< .001
	Robust mean absolute deviation	-2.693	.007
	Mean absolute deviation	-3.046	.002
	Total energy	-2.870	.004
Gray level run length matrix	Short run low gray level emphasis	-3.311	.001
	Gray level variance	-3.046	.002
	Low gray level run emphasis	-3.311	.001
	Gray level nonuniformity normalized	-2.958	.003
Gray level size zone matrix	Gray level variance	-3.046	.002
	Gray level nonuniformity normalized	-3.046	.002
	Size zone nonuniformity	-3.400	.001
	Small area high gray level emphasis	-1.987	.047
Neighboring gray tone difference matrix	Coarseness	-2.870	.004
	Complexity	-3.135	.002

rejection. The brightness, contrast, homogeneity, and signal-to-noise ratio changes are parameters sensitive to the disease intensity in rejected kidneys [13]. The authors have proposed

that this method may be a new, noninvasive method to evaluate and monitor kidney transplantation. Some of the isolated features differed significantly between rejected and nonrejected kidneys. So far, ultrasound texture analysis studies have been conducted, which showed a statistically significant correlation between some texture parameters and the rejection of the transplanted kidney [13]. On the other hand, the researchers who dealt with kidney textural analysis of MRI images [2] focused their attention on the first-order method, where a correlation between textural parameters and height-adjusted total kidney volume and eGFR was also found in chronic kidney disease progression.

The main limitation of our study was, owing to the small study group, we were not able to perform the analysis of textural analysis in comparison to kidney biopsy findings. Identifying parameters associated with histopathological findings strongly enough to be helpful in clinical decision making will be of high interest and will have potential clinical applications. Therefore, it is advisable to conduct further texture studies in MRI images to expand the possibilities for noninvasive diagnosis of transplanted kidneys. The influence of various factors on texture parameters needs to be studied in-depth, and the image processing and analysis process needs to be optimized.

CONCLUSIONS

Our preliminary research shows the association between some texture features with eGFR, which makes textural analysis a promising tool for the assessment of transplanted kidney function. However, this promising method of image processing needs further studies to determine the effect of binning, ROI size, and placement of ROI in the organ.

REFERENCES

[1] Ardakani AA, Mohammadi A, Najafabad BK, Abolghasemi J. Assessment of kidney function after allograft transplantation by texture analysis. Iran J Kidney Dis 2017;11: 157e64.

[2] Kline TL, Korfiatis P, Edwards ME, Bae KT, Yu A, Chapman AB, et al. Image texture features predict renal function decline in patients with autosomal dominant polycystic kidney disease. Kidney Int 2017;92:1206e16. https://doi.org/10.1016/j.kint. 2017.03.026.

[3] Nioche C, Orlhac F, Boughdad S, Ruezé S, Goya-Outi J, Robert C, et al. LIFEX: a freeware for radiomic feature calculation in multimodality imaging to accelerate advances in the characterization of tumor heterogeneity. Cancer Res 2018;78:4786e9. https://doi.org/10.1158/0008-5472.CAN-18-0125.

[4] Ford J, Dogan N, Young L, Yang F. Quantitative radiomics: impact of pulse sequence parameter selection on MRI-based textural features of the brain. Contrast Media Mol Imaging 2018: 1729071. https://doi.org/10.1155/2018/1729071.

[5] Goya-Outi J, Orlhac F, Calmon R, Alentorn A, Nioche C, Philippe C, et al. Computation of reliable textural indices from multimodal brain MRI: suggestions based on a study of patients with diffuse intrinsic pontine glioma. Phys Med Biol 2018;63: 105003. https://doi.org/10.1088/1361-6560/aabd21.

[6] Materka A. Texture analysis methodologies for magnetic resonance imaging. Dialogues Clin Neurosci 2004;6:243e50.

[7] Castellano G, Bonilha L, Li LM, Cendes F. Texture analysis of medical images. Clin Radiol 2004;59:1061e9. https://doi.org/10.1016/j.crad.2004.07.008.

[8] Tustison NJ, Avants BB, Cook PA, Zheng Y, Egan A, Yushkevich PA, et al. N4ITK: improved N3 bias correction. IEEE Trans Med Imaging 2010;29:1310e20. https://doi.org/10.1109/TMI.2010.2046908.

[9] van Griethuysen JJM, et al. Computational radiomics system to decode the radiographic phenotype. American Association for Cancer Research 2017;77(21). https://doi.org/10.1158/0008-5472. CAN-17-0339. Kickingereder P, Burth S, Wick A, Götz M, Eidel O, Schlemmer HP, et al. Radiomic profiling of glioblastoma: identifying an imaging predictor of patient survival with improved performance over established clinical and radiologic risk models. Radiology 2016;280:880e9. https://doi.org/10.1148/radiol.2016160845.

[10] de Leon AD, Kapur P, Pedrosa I. Radiomics in kidney cancer: MR imaging. Magn Reson Imaging Clin N Am 2019;27: 1e13. https://doi.org/10.1016/j.mric.2018.08.005.

[11] Abbasian Ardakani A, Mohammadi A, Khalili Najafabad B, Abolghasemi J. Assessment of kidney function after allograft transplantation by texture analysis. Iran J Kidney Dis 2017;11: 157e64.

[12] Kee TYS, Chapman JR, O′Connell PJ, Fung CLS, Allen RDM, Kable K, et al. Treatment of subclinical rejection diagnosed by protocol biopsy of kidney transplants. Transplantation 2006;82:36e42. https://doi.org/10.1097/01.tp.0000225783.86950.c2.

Article

Textural Analysis of Magnetic Resonance Images as an Additional Evaluation Tool of Parotid Glands in Sjögren—Primarily Findings

Małgorzata Grzywińska [1,2,*], Magdalena Karwecka [2], Anna Pomorska [3], Ninela Irga-Jaworska [3], Dominik Świętoń [2,4]

[1] Neuroinformatics and Artificial Intelligence Lab, Department of Neurophysiology, Neuropsychology and Neuroinformatics, Medical University of Gdansk, 80-210 Gdansk, Poland

[2] Department of Radiology, University Clinical Center, 80-952 Gdansk, Poland; dominik.swieton@gumed.edu.pl (D.S.)´

[3] 2nd Department of Pediatrics, Haemathology & Oncology, Medical University of Gdansk, 80-210 Gdansk, Poland

[4] 2nd Department of Radiology, Medical University of Gdansk, 80-210 Gdansk, Poland

* Correspondence: malgorzata.grzywinska@gumed.edu.pl

Abstract: Magnetic Resonance Imaging (MRI) plays a leading role in diagnosing soft tissue pathologies, especially in the head and neck. It is increasingly popular for evaluating salivary gland issues like neoplasms and Sjogren's Syndrome. Advanced MRI methods, including MRI sialography and texture analysis, offer non-invasive alternatives, enhancing MRI's role. This study focused on the relationship between the apparent diffusion coefficient (ADC) and T2-weighted MRI sialography and texture analysis (TA) of parotid glands in children with and without Sjogren's Syndrome (SS). Using 3.0 Tesla MRI with DWI and T2-weighted imaging, expended texture analysis, first-order statistics (FSOs), second-order, and higher-order statistics were conducted. The results showed significant differences in parotid ADC values, with lower values in the SS group, particularly in cases of higher disease activity. Lower kurtosis values were associated with more severe Tonami Scale grades. FSO parameters correlated well with the texture analysis from T2-weighted images, indicating promise in grading parotid gland inflammation. However, further research is needed to understand the impact of variables like binning and region of interest (ROI) size. This study highlights the potential of texture analysis for assessing parotid gland inflammation and emphasizes the need for more investigations in this area.

Keywords: Sjögren's syndrome (SS); texture analysis (TA); radiomics

Introduction

The diagnosis and treatment of Sjögren's Syndrome (SS), a complicated autoimmune illness, establish unique difficulties, especially in the case of children. Since the symptoms of SS in children approaches used to diagnose SS in children, particularly those that rely on immunologic characteristics. Additionally, clinical signs may not last long.

One promising approach is imaging methods, which offer the advantage of being non-invasive and can provide additional information about the extent and characteristics of SS-related changes within the affected organs. Among these imaging techniques, salivary gland ultrasound stands out as a promising screening tool with the potential to

are nonspecific and are usually accompanied by a delayed diagnosis, it is essential to identify the disease early and evaluate its activity. As reported in the literature [1], SS can present itself in various ways, impacting not just the salivary and lacrimal glands but also influencing other organs such as the joints, lungs, kidneys, veins, and muscles. A formal diagnosis of SS in children is complicated by the lack of SS criteria dedicated to children. The latest 2016 ACR/EULAR criteria for SS used in adults are often not adequate for the onset of disease in children [2]. Although these criteria can be used in diagnosis, the opinion of an experienced specialist dealing with patients with SS remains crucial in establishing a diagnosis of SS in children.

Considering the complexity of the illness, finding suitable and non-invasive diagnostic methods is needed. However, limited sensitivity is a common problem with conventional

replace invasive salivary gland biopsy in the diagnostic process [3]. However, it is important to note that the absence of a validated assessment system and the natural variability between sonographers present significant challenges in achieving objective and consistent monitoring using this method.

Another common imaging approach in SS diagnosis is sialography, which relies on radiographic strategies to observe anatomical changes in the salivary gland duct system. In contrast, scintigraphy offers valuable data by measuring the rate and intensity of technetium-99m (99mTc) uptake in the mouth after intravenous infusion, providing insights into salivary gland function. Despite their utility, both methods are invasive and carry the risk of radiation exposure side effects, making them less than ideal for pediatric patients [4].

MRI with a sialography sequence is an effective alternative method that, unfortunately, is underappreciated [5]. This approach takes advantage of the multi-parametric nature of MRI, allowing for the assessment of gland inflammation, structure, and function [6,7]. The relatively new field of the textural analysis of MR images holds promise in enhancing the diagnostic process.
Texture analysis in the context of MRI involves the quantitative assessment of spatial patterns of signal intensity changes within a specific region of interest. It comprises various techniques for quantifying the image's gray-level patterns and voxel relationships. These textural parameters are loaded sources of information, offering insights into the region's heterogeneity, often showing microstructural changes. Recent research suggests that individual texture characteristics can be optimally combined with dynamic disease progression indicators, offering new dimensions for diagnosing and monitoring diseases. Prior studies have demonstrated the high accuracy of texture analysis in differentiating between SS patient grades based on apparent diffusion coefficient (ADC) values in adults [8,9]; however, there remains a gap in standardized methods for texture assessment. Some studies have explored diverse approaches to analyzing MR images for diagnostic purposes in SS [10,11], emphasizing the need for a unified framework for texture assessment in the context of this challenging disease.

Sjögren's Syndrome in pediatric patients causes unique diagnostic challenges due to its nonspecific and often delayed clinical presentation. Traditional diagnostic methods lack the sensitivity for early detection. Imaging methods, including salivary gland ultrasound, sialography, and scintigraphy, offer valuable insight but have essential limitations and risks. MRI with sialography, while effective, is underused. A texture analysis of MR images is a promising possibility for improving the diagnostic process, offering quantitative insights into SS's microstructural and dynamic aspects.

2. Materials and Methods

2.1. Research Group

The Independent Bioethics Committee for Scientific Research at the Medical University of Gdansk provided ethical approval for this study (NKBBN/228/2021). All participants (above 16 years) or legal guardians (under 16 years) gave written consent to participate in the examination, depending on the participant's age, as below:

1. For participants above 16 years, informed consent was obtained from all for study participation.
2. For participants below 16 years, informed consent was obtained from all of the parents or legal guardians for study participation.

The research was conducted according to the Declaration of Helsinki of 1975, which was subsequently revised in 2000. All analysis images were obtained with consent from all of the subjects and were safeguarded throughout the study.

A total of 36 patients were included in the primary analysis, all of whom met the inclusion criteria of having a positive small labial salivary gland biopsy for Sjögren's Syndrome (SS). These patients underwent routine clinical control. The age of the patients ranged from 5 to 20 years old. The mean age of the patient group was 12.5 years old, with a median of 12 years old. The patient group consisted of 16 males and 20 females, and the interquartile range (IQR) of their ages was 5.

Conversely, the control group included 20 children or young adolescents, with a mean age of 13.5 and a median age of 14. There were 12 males and 8 females in the control group, and the interquartile range (IQR) of their ages was 4.

The patients' demographic information is shown in Table 1, which provides further details on the characteristics of the study participants.

Table 1. The demographic characteristics of patients.

Index		Value SS Group	Value Healthy Group
Age	n.a.*	12.5 ± 3.4 yrs	13.5 ± 2.4 yrs
Gender	female	20	8
	male	16	12
Tonami scale	0	12	n.a.
	1	8	n.a.
	2	30	n.a.
	3	22	n.a.

* n.a.—not applicable.

2.2. MRI Examination

The examinations in this study were performed using a Philips Achieva 3T TX magnetic resonance scanner (Philips Healthcare, Best, The Netherlands). To enhance the imaging precision of the head–neck region assessment, a 16-channel neurovascular coil was used.

The examination protocol included a survey sequence and a set of three-plane, low resolution, large field-of-view (FOV) images designed to precisely localize the specific anatomical region under examination. This is a crucial step in imaging to focus on the intended area of interest.

Following the survey sequence, morphological sequences were performed in three planes. This sequence provides the necessary anatomical orientation for salivary glands. It is important to highlight that these sequences were chosen for their suitability in our analysis and for clinical assessment.

The primary sequences that formed the foundation of our analysis included two essential imaging techniques:

1. Diffusion-weighted imaging (DWI) is sensitive to the movement of water molecules within tissues. It offers a valuable understanding of the tissue microstructure and helps identify areas of restricted diffusion, which can specify various pathological conditions.
2. T2-weighted imaging offers exceptional contrast for visualizing different types of tissues, making this type of sequence helpful in identifying anatomical structures and pathological changes. This image can highlight areas of edema and inflammation, which can be highly important in the context of diseases like Sjögren's Syndrome.

The combination of these sequences (along with the other morphological imaging sequences mentioned in Table 2) formed the basis of our analysis. This allowed a comprehensive evaluation of the anatomical and pathological aspects related to the patients in the study and played a fundamental role in understanding Sjögren's Syndrome in the pediatric population of our study.

Table 2. MRI protocol.

Sequence	FOV (mm)	Slice Thickness/Gap (mm)	Voxel (mm)	Suppress Fat	Flip Angle	Number of Averages	TE/TR (ms)	Matrix	Plane
Survey/localizer	250/250	10	0.98 × 1.95 × 10	-	15	1	4.6/11	256	Coronal, transverse, sagittal
T2_TSE	210/210	3/0.5	0.80 × 1.15 × 3	-	90	2	90/2500	512	Coronal
T2_TSE	240/240	3/0.6	0.70 × 0.87 × 3	-	90	2	90/3000–4500	640	Transverse
T2_STIR	210/210	3/0.6	0.78 × 0.98 × 3	STIR	-	2	90/1400–4000	560	Transverse
3D_TSE_SPIR_obligue	300/245/48	2	1 × 1.24 × 2	SPIR	90	2	90/120	1008	Sagittal
mDIXON	250/250/130	1	1 × 1 × 2	-	10	3	Shortest/shortest	256	Transverse
DWI	240/240	4.5/1	1.5 × 2.18 × 4.5	SPIR	90	1	Shortest/shortest	288	Transverse

TSE—Turbo Spin Echo; SPAIR—Spectral Presaturation with Inversion Recovery; 3D TSE SPIR imaging—3D Turbo Spin Echo Spectral Presaturation with Inversion Recovery imaging—Sialography; mDixon—time-consuming acquisition of in-phase and opposed-phase gradient-echo images; STIR—Short-TI Inversion Recovery; T2—the time constant for decay/dephasing of transverse magnetization; DWI—Diffusion-weighted Imaging.

2.3. Image Analysis

The MR images were reviewed by a qualified radiologist who evaluated the image findings. The MR images were determined according to the high T2 signal intensity size through all areas of glands in the MR sialography sequence. This made it possible to evaluate the state of the salivary glands in a way that was both thorough and objective, based only on the radiological features shown in the MR images.

The Tonami modified criteria were as below [12]:

1. Grade 0 (normal)—no evidence;
2. Grade 1 (punctate)—areas ≤ 1 mm in diameter;

3. Grade 2 (globular)—1–2 mm in diameter;
4. Grade 3 (cavitary)—up to 1 cm in diameter;
5. Grade 4 (destructive)— complete destruction of the gland parenchyma.

The ADC maps (apparent diffusion coefficient maps) were automatically generated from DWI (b = 0.500 and 1000 s/mm^2) scans by the manufacturing software (R5.3, Philips Healthcare, Best, The Netherlands), which was integrated with the workstation using the monoexponential model [11]:

$$S = S_0 \cdot e^{-b \cdot ADC}$$

To correct the field inhomogeneity, we used a specialized correction algorithm known as the N4 algorithm [13]. This algorithm is designed to alleviate distortion caused by inhomogeneity in magnetic field strength within the image data. This can enhance the quality and accuracy of the analysis. Following the field inhomogeneity correction, a texture analysis using package pyRadiomics (v3.0.1) was performed (with specific reference to the Radiomics modules [14]). We set particular parameters, like absolute bound and bin width, to ensure the consistency and reliability of the analysis.

The region of interest (ROI) was drawn manually, covering all glands. Additionally, to minimize any potential influence from surrounding tissues or artifacts at the periphery of the glands, we kept approximately 1 mm distance from the edge when drawing the ROI.
The ROI was drawn in all volumes of each parotid in ADC maps and T2 sequences.

The texture features obtained from these regions of interest (ROIs) following formulas were divided into subgroups [15] (Figure 1):

1. First-order statistic (FSO), including Energy, Total Energy, Entropy, Minimum, 10th percentile, 90th percentile, Maximum, Mean, Median, Interquartile Range, Range, Mean Absolute Deviation (MAD), Robust Mean Absolute Deviation (rMAD), Root Mean Square (RMS), Standard Deviation, Skewness, Kurtosis, Variance, Uniformity;
2. Gray Level Co-occurrence Matrix (GLCM) features, including Joint Average, Cluster Prominence, Cluster Shade, Cluster Tendency, Contrast, Correlation, Difference Average, Difference Entropy, Difference Variance, Joint Energy, Joint Entropy, Informational Measure of Correlation 1 and 2 (IMC), Inverse Difference Moment (IDM), Maximal Correlation Coefficient (MCC), Inverse Difference Moment Normalized (IDMN), Inverse Difference (ID), Inverse Difference Normalized (IDN), Inverse Variance, Maximum Probability, Sum Average, Sum Entropy, Sum of Squares;
3. Gray Level Size Zone Matrix (GLSZM) features, including Small Area Emphasis (SAE), Large Area Emphasis (LAE), Gray Level Non-Uniformity (GLN), Gray Level NonUniformity Normalized (GLNN), Size-Zone Non-Uniformity (SZN), Size-Zone NonUniformity Normalized (SZNN), Zone Percentage (ZP), Gray Level Variance (GLV), Zone Variance (ZV), Zone Entropy (ZE), Low Gray Level Zone Emphasis (LGLZE), High Gray Level Zone Emphasis (HGLZE), Small Area Low Gray Level Emphasis (SALGLE), Small Area High Gray Level Emphasis (SAHGLE), Large Area Low Gray Level Emphasis (LALGLE), Large Area High Gray Level Emphasis (LAHGLE);

4. Gray Level Run Length Matrix (GLRLM) features, including Short Run Emphasis (SRE), Long Run Emphasis (LRE), Gray Level Non-Uniformity (GLN), Gray Level Non-Uniformity Normalized (GLNN), Run Length Non-Uniformity (RLN), Run Length Non-Uniformity Normalized (RLNN), Run Percentage (RP), Gray Level Variance (GLV), Run Variance (RV), Run Entropy (RE), Low Gray Level Run Emphasis (LGLRE), High Gray Level Run Emphasis (HGLRE), Short Run Low Gray Level Emphasis (SRLGLE), Short Run High Gray Level Emphasis (SRHGLE), Long Run Low Gray Level Emphasis (LRLGLE), Long Run High Gray Level Emphasis (LRHGLE);
5. Neighboring Gray Tone Difference Matrix (NGTDM) features, including Coarseness, Contrast, Busyness, Complexity, Strength;
6. Gray Level Dependence Matrix (GLDM) features, including Small Dependence Emphasis (SDE), Large Dependence Emphasis (LDE), Gray Level Non-Uniformity (GLN), Dependence Non-Uniformity (DN), Dependence Non-Uniformity Normalized (DNN), Gray Level Variance (GLV), Dependence Variance (DV), Dependence Entropy (DE),

   Low Gray Level Emphasis (LGLE), High Gray Level Emphasis (HGLE), Small Dependence Low Gray Level Emphasis (SDLGLE), Small Dependence High Gray Level Emphasis (SDHGLE), Large Dependence Low Gray Level Emphasis (LDLGLE), Large Dependence High Gray Level Emphasis (LDHGLE).

2.4. Statistical Analysis

A statistical analysis was performed using SPSS Statistics 27 (IBM, Armonk, NY, USA). We assessed the normality of all results, and the Shapiro–Wilk test showed that none of the parameters followed a normal distribution. Therefore, we employed the Spearman correlation test to examine the relationships between the collected data and identify correlations between texture features in diseased and healthy glands. We applied the independent-samples Kruskal–Wallis test to compare group differences among the glands. Afterward, a post hoc analysis was performed to determine which groups showed significant differences, with a significance of $p < 0.05$.

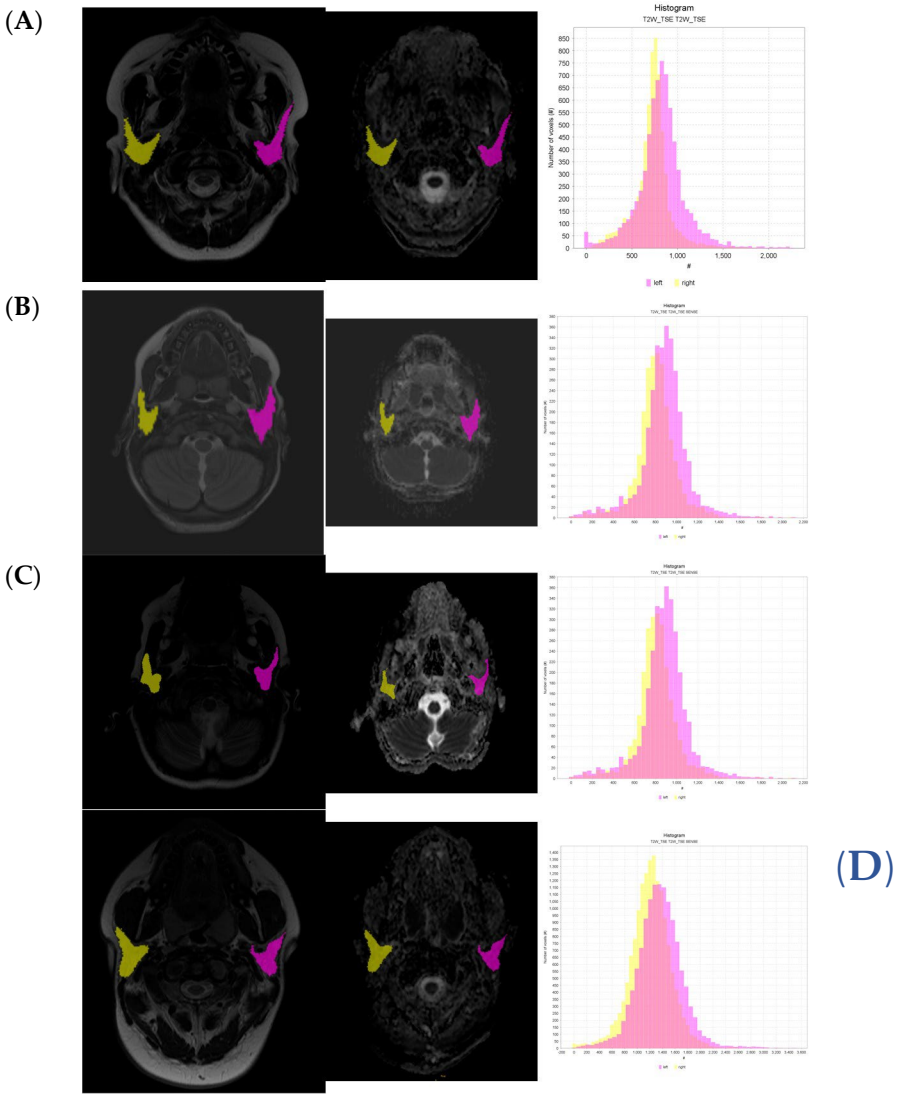

Figure 1. Axial images of T2-weighted imaging, diffusion-weighted imaging (DWI), and apparent diffusion coefficient (ADC). Histogram correlated with T2 images. For Tonami scale: (**A**) grade 0, (**B**) grade 1, (**C**) grade 2, (**D**) grade 3.

3. Results

3.1. MRI Sialography Grades by the Tonami Scale

We assessed the MRI sialography grades for each gland, considering the presence of cystic changes [12]. Our findings indicated that grade 0 was observed in 12 glands (16%), grade 1 in 8 glands (11%), grade 2 in 30 glands (42%), and grade 3 in 22 glands (31%)

(Table 1).

3.2. ADC Values

The value of the ADC from Sjögren's Syndrome patients and the control group was obtained from the ROI in each gland; the mean ADC value depending on the MRI morphology grade is present in Table 3 (grade 0—0.88 ± 0.14; grade 1—0.86 ± 0.09;

grade 2—0.97 ± 0.17; grade 3—1.04 ± 0.19 [10^{-3} mm $\frac{2}{s}$]). The ADC value from the control group: 1.04 ± 0.10 . There was a significant difference (using the independent-samples Kruskal–Wallis test: $X^2(4) = 25.139$, $p < 0.001$) of the ADC value relative to MRI morphology grades (Tonami scale [12]) (Figure 2). Therefore, further analyses were performed with a pairwise comparison with Bonferroni correction. An obtained significant difference ($p < 0.05$) between groups (Table 3) was

- 1–healthy ($p = 0.005$),
- 1–3 ($p = 0.046$),
- 0–3 ($p = 0.035$),
- 0–healthy ($p = 0.001$).

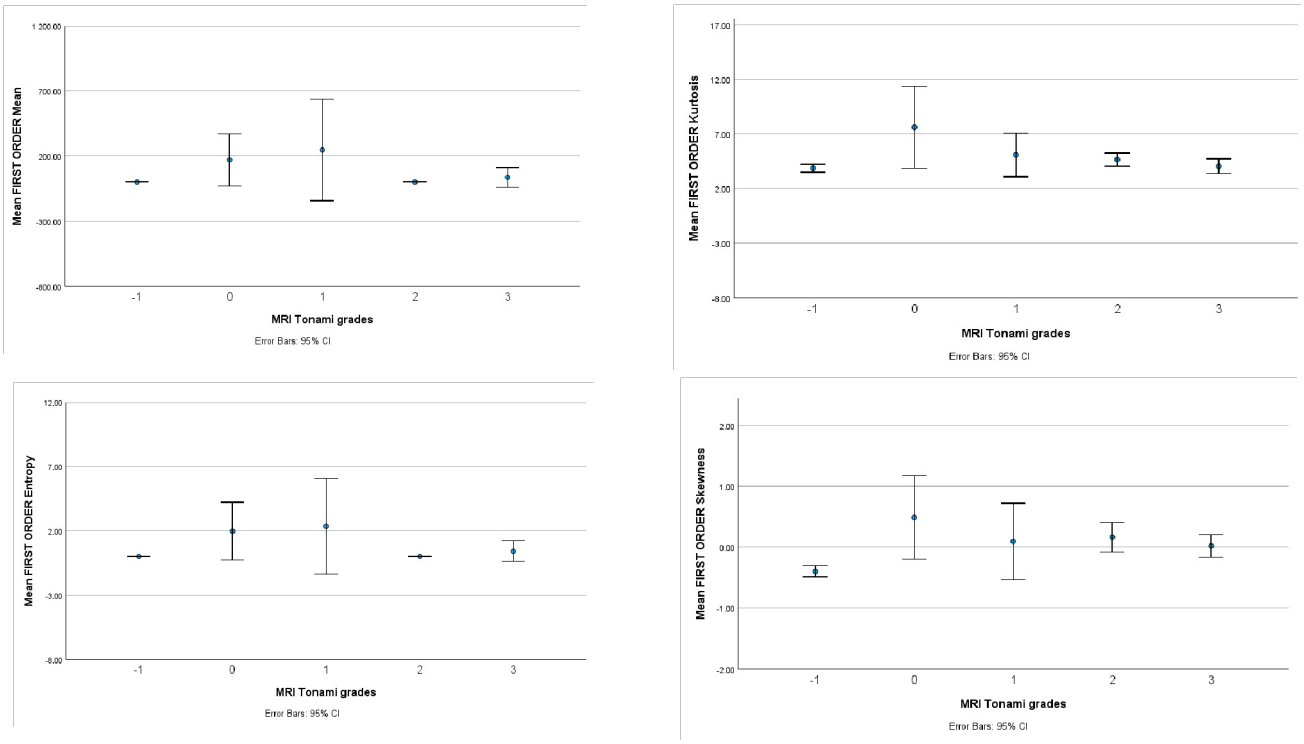

Figure 2. Graphic presents the value of first-order statistics from ADC depending on MRI Tonami's grades.

Table 3. Mean values of image and texture analysis of ADC images compared to MRI Tonami grades.

Parameters	Tonami Scale									
	Healthy		0		1		2		3	
	Mean	Std. Deviation	Mean	Std. Deviation	Mean	Std. Deviation	Mean	Std. Deviation	Mean	Std. Deviation
Mean [10^{-3} mm²/s]	1.04	0.10	0.88	0.14	0.86	0.09	0.97	0.17	1.04	0.19
Median [10^{-3} mm²/s]	1.06	0.10	0.86	0.14	0.88	0.09	0.96	0.17	1.03	0.19
Entropy	0.01	0.00	2.95	4.05	5.46	4.74	0.04	0.01	0.97	0.27
Kurtosis	3.86	1.19	9.24	6.63	6.48	1.97	5.03	0.35	1.23	0.17
Skewness	−0.39	0.28	0.99	0.09	0.57	0.07	0.36	0.07	0.17	0.03

3.3. Whole-Volume ADC Image for Texture Analysis

A whole-volume ADC analysis was computed for each gland without distinguishing between the left and right glands. As presented in Table 3, a moderate correlation was observed between texture features and MRI morphology grades. Notably, a prevalent positive correlation was found between MRI-positive sialography and nearly every

texture parameter with higher statistical attributes. On the contrary, a negative correlation was observed for first-order statistics (FSOs), including skewness, kurtosis, and entropy.

The parotid ADC values from the whole-volume region of interest (ROI) were significantly lower in group 1 on the Tonami scale than in groups with more advanced changes. This difference was confirmed by a Kruskal–Wallis H test, demonstrating statistical significance ($p > 0.05$). Furthermore, pairwise comparisons of the Tonami Scale for groups 1–2 and 1–3 revealed significant differences (as indicated in Table 3). Notably, the most critical finding in this research is the statistically significant difference between grade 0 and the healthy group and grade 3, with significance noted as $p < 0.05$.

3.4. Whole-Volume T2 for Texture Analysis

Each salivary gland was analyzed without differentiating between the left and right glands. This method made it possible to thoroughly evaluate the texture properties and how they relate to the MRI morphological grades. Table 4 summarizes the findings and indicates a moderate correlation between the MRI morphological grades and the obtained texture features. This result suggests that the textural characteristics obtained from the imaging data are meaningful and can highlight the structural and compositional changes inside the salivary glands.

Table 4. Mean values of image and texture analysis of T2 images compared to MRI Tonami grades.

Texture Parameters	Tonami Scale									
	Healthy		0		1		2		3	
	Mean	Std. Deviation	Mean	Std. Deviation	Mean	Std. Deviation	Mean	Std. Deviation	Mean	Std. Deviation
Median	891.53	244.23	698.58	252.43	890.44	481.32	849.78	344.92	897.32	300.99
Entropy	7.51	1.76	8.21	0.44	8.48	0.49	8.49	0.69	8.72	0.70
Kurtosis	4.79	1.57	7.33	3.58	4.89	0.68	6.02	1.56	5.24	1.78
Mean	887.56	242.88	697.16	246.50	880.58	451.04	850.80	345.87	911.03	303.55
GLDM_Dependence NonUniformity	5791	3201	13,600	669	11,600	2390	13,400	7720	14,200	6530
GLDM_Small Dependence High Gray Level Emphasis	95,569	563,232	115,000	887,000	203,000	202,000	191,000	162,000	209,000	144,000
GLCM_Imc1	−0.32	0.09	−0.27	0.06	−0.31	0.07	−0.32	0.08	−0.34	0.06
GLRLM_Run Entropy	7.67	1.21	8.26	0.43	8.53	0.48	8.53	0.67	8.76	0.68
GLSZM_Zone Entropy	8.11	1.19	8.69	0.38	8.89	0.37	8.92	0.54	9.07	0.58

A positive and moderate correlation was found between individual MRI morphology parameters and some specific texture parameters, specifically the first-order statistics (FSOs) parameters (Table 4). This positive correlation indicates that the FSO parameters, which characterize basic statistical features of the images, can effectively capture significant details about the structural features of the gland, as seen in the MR images.

4. Discussion

The texture analysis of images is a complex process that involves the assessment of various spatial relationships and characteristics within the image. The set of texture

features we have examined, including Small Dependence Emphasis (SDE), Large Dependence

Emphasis (LDE), Gray Level Non-Uniformity (GLN), Dependence Non-Uniformity (DN),

Dependence Non-Uniformity Normalized (DNN), Gray Level Variance (GLV), Dependence

Variance (DV), Dependence Entropy (DE), Low Gray Level Emphasis (LGLE), High Gray Level Emphasis (HGLE), Small Dependence Low Gray Level Emphasis (SDLGLE), Small Dependence High Gray Level Emphasis (SDHGLE), Large Dependence Low Gray Level Emphasis (LDLGLE), and Large Dependence High Gray Level Emphasis (LDHGLE), collectively provide valuable insights into the textural characteristics of an image.

This primary study examines salivary gland texture in MR images within a pediatric Sjogren Syndrome (SS) cohort. The research investigates the differences in textural characteristics within two regularly acquired MR images in SS patients—ADC maps and T2-weighted images. In total, 36 patients were included in the analysis, with each salivary gland analyzed individually (N = 72). For the control group, 20 examinations were conducted, examining 40 glands.

A critical objective of this study was to identify the most suitable MR image type for grading disease severity using texture analysis. The Tonami scale for MRI positive sialography served as the standard for comparing data derived from texture analysis. Information was extracted from the intensity of each voxel within the region of interest (ROI) covering the entire gland volume (with the 1 mm margin).

The parotid ADC values from whole volume ROIs were significantly lower in the Tonami scale grades 0 and 1 than in the high-activity group (grade 3 and above). Notably, the average ADC value in the reference group displayed a significant difference to grade

1. This could suggest that the ADC, often used as an inflammatory marker, can help in promptly diagnosing early-stage SS (grade 1). These findings indicate that higher sialography grades correspond to elevated ADC values [9,16,17].

Moreover, lower kurtosis and skewness values were observed in the highest Tonami Scale grade, which is recognized to likely increase tissue heterogeneity due to atrophy, fibrotic tissue replacement, and fluid-filled sialectasis. This condition influences the tissue structure, resulting in advanced changes. Unlike previous studies [10,18,19] in adults, unchanged or minimally affected glands in MRI sialography exhibited a notable decrease in ADC values, which is indicative of an ongoing inflammatory process preceding structural remodeling (Figure 2 and Table 5). This discovery reinforces the ability of an early-stage diagnosis of pediatric SS, which involves a particularly challenging population [2].

Table 5. Pairwise comparisons of ADC values with MRI Tonami grades.

Sample 1–Sample 2	Test Statistic	Std. Error	Std. Test Statistic	Sig.	Adj. Sig. [a]
1–3	−39.756	14.033	−2.833	0.005	0.046
1–healthy	46.178	13.180	3.504	<0.001	0.005
0–3	−33.905	11.605	−2.922	0.003	0.035
0–healthy	40.327	10.558	3.820	<0.001	0.001

Each row tests the null hypothesis that the Sample 1 and Sample 2 distributions are the same. Asymptotic significances (2-sided tests) are displayed. The significance level is 0.050. [a] Significance values have been adjusted by the Bonferroni correction for multiple tests.

In the T2 image texture analysis, the first-order statistic (FSO) parameters displayed a moderate correlation among individual parameters. However, lower kurtosis values were observed in the highest activity SS group on the Tonami Scale. Entropy values remained relatively consistent across all grades, potentially due to lower sensitivity to inflammation than the DWI sequence. Nevertheless, this characteristic upholds high repeatability and minimizes artifacts, benefiting this sequence more. A T2-weighted MR image signal intensity primarily decreases from intracellular and extravascular space, showing acute inflammation which is often associated with SS disease activity [10,18].

These texture features collectively offer a comprehensive tool for quantifying and understanding the textural content of images, allowing their application in medical imaging for tasks ranging from quality control to disease diagnosis. The choice of which features to use will depend on the specific image analysis task and the nature of the texture patterns of interest [20–23].

Despite these insightful findings, several limitations need consideration. The small sample size in this, inherent to the pediatric nature of the group, should be acknowledged. Ensuring an optimal MRI protocol and addressing field inhomogeneity correction are crucial. Additionally, future studies should explore excluding signals from cysts in high-grade SS, which can artificially elevate ADC map signals. These limitations need further investigation.

Moreover, the potential link between histological activity and basic, unfiltered texture parameters on T2-weighted images and ADC maps may be fundamental to evaluating disease activity. Combining both sequences could address issues concerning signal-tonoise ratio and volume averaging in ADC maps. Textural analysis alongside sialography sequences and ADC maps presents a novel approach to early-stage SS diagnosis in children and improves disease monitoring.

The recent review of Wenxing Zhong et al. [24] emphasizes the efficacy of magnetic resonance imaging (MRI) in evaluating gland structure, size, and abnormalities such as atrophy, inflammation, and fibrosis. MRI plays a role in disease monitoring and treatment assessment, particularly with recent techniques like dynamic contrast-enhanced MRI, diffusion-weighted imaging, and radiomics. They reference the adult study by Muntean et al., which reported a 91% sensitivity and 83% specificity in radiomics analysis [25]. In our opinion, MRI might find a place in the diagnostic criteria of SS, especially in the pediatric population. According to our results, MRI improves diagnostic precision in diagnosing early stages of the disease, potentially eliminating biopsy from the diagnostic algorithm. Before inclusion, it would be necessary to carefully evaluate standardization, repeatability, and association with clinical results in larger groups.

It is worth mentioning the historical context of Sjögren's Syndrome and Mikulicz Syndrome; the conventional approach to managing these conditions involved bilateral parotidectomy as a primary solution. However, this method occasionally led to complications such as Frey syndrome, characterized by gustatory sweating. Notably, Freni et al. [26] demonstrated the successful use of botulinum toxin in addressing Frey syndrome, offering an alternative to the traditional surgical approach [26,27]. Finding a way to improve disease monitoring and prevent invasive treatment methods is crucial. Nevertheless, in the case of children who do not exhibit dryness symptoms, objective dryness, or SS antibodies, an additional investigation, including salivary gland imaging and histopathological assessment, must assist in confirming the diagnosis [4]. It suggests that many children with recurrent or persistent salivary gland enlargement of unknown origin are likely to receive an SS diagnosis following a comprehensive workup. However, not meeting existing adult SS criteria does not exclude the diagnosis of SS [2,28]. Continued observation with periodic repeat testing (imaging, serological, functional) to evaluate for progression to SS is crucial for these children.

Further research and cooperative efforts are reasonable to explore the feasibility and reliability of integrating MRI findings into the diagnostic framework for SS [25]. The future of textural analyses of salivary glands in Sjögren's Syndrome could be linked to artificial intelligence (AI). It could hold significant promise for advancing research and clinical applications, contributing first to segmentation and performing detailed quantitative analyses of textural features in salivary gland images. AI can provide a more objective and consistent analysis, contributing to a deeper understanding of Sjögren's Syndrome manifestations. The other side of using AI is pattern recognition, but it will require a large dataset to recognize these patterns. Furthermore, AI has the potential to be one of the most important aspects in accelerating the pace of research and enhancing diagnostic accuracy.

5. Conclusions

The complex nature of Sjögren's Syndrome, its various clinical presentations, and the difficulties related to traditional diagnostic methods highlight the significance of investigating innovative approaches like textural analyses of MRI.

This study shows different areas in which textural analysis can improved, like:

1. Early diagnosis of Sjögren's Syndrome (grade 1): One of the most significant implications of this study is the prospect of early diagnosis of Sjögren's Syndrome, especially in children. This is crucial because Sjögren's Syndrome is known for its nonspecific symptoms in the early stage of inflammation. Using MRI-based texture analysis, we can detect subtle changes at a microstructural level within parotid glands, which allows us to identify Sjögren's Syndrome in the early stages. This can lead to prompt intervention and a better prognosis for young patients.
2. Monitoring of remodeling salivary glands in the process of Sjögren's Syndrome: Because Sjögren's Syndrome is characterized by the progressive remodeling and destruction of the salivary glands, texture analysis can be a valuable tool for monitoring these changes over time by quantifying the heterogeneity and eventual microstructural changes in the glands. Our study suggests that we can track the disease's progression and possible impact on the glandular tissue. This information will significantly impact the individual treatment strategy and therapeutic intervention.
3. Reducing radiation exposure: Traditional diagnostics like sialography and scintigraphy can be replaced by magnetic resonance imaging only. This can be a safer approach for the pediatric population.
4. Treatment planning can be more individualized: The ability to assess microstructures through textural analysis can be essential for better understanding the characteristics of each patient's condition.

In conclusion, textural analyses of MR images for evaluating Sjögren's Syndrome hold great promise, especially in childrens' diagnostics. It has the potential to offer a non-invasive, precise, and patient-centric approach. This primary research explores the full potential of textural analysis and defines our understanding of its significance in clinical practice.

Author Contributions: Conceptualization, M.G. and D.S.; methodology, M.G. and D.´ S.; validation,´ M.G. and D.S.; formal analysis, M.G.; data curation, M.G., M.K., A.P., N.I.-J., and D.´ S.; writing—´ original draft preparation, M.G.; writing—review and editing, M.G., D.S., M.K., A.P., and N.I.-J.;´ visualization, M.G.; supervision, D.S.; project administration, M.G. All authors have read and agreed´ to the published version of the manuscript.

Funding: The National Science Center—NCN 2020/04/X/NZ5/00599 (data April 2020) provided funding for the MRI examination.

Institutional Review Board Statement: This study received approval from the Independent Bioethics Committee for Scientific Research at the Medical University of Gdan´sk (NKBBN/228/2021).

Informed Consent Statement: For participants above 16 years, informed consent was obtained from all the participants for study participation. For participants below 16 years, informed consent was obtained from

all of the parents and/or legal guardians for study participation. The research was conducted according to the Declaration of Helsinki of 1975, as revised in 2000. All analysis images

were obtained, respectively, with consent from all subjects.

Data Availability Statement: The data presented in this study are available on reasonable and qualified research request from the corresponding author. Data requestors will need to sign a data access agreement.

Conflicts of Interest: The authors declare no conflict of interest. The funders had no role in the design of the study; in the collection, analyses, or interpretation of data; in the writing of the manuscript; or in the decision to publish the results.

References

1. Stefanski, A.-L.; Tomiak, C.; Pleyer, U.; Dietrich, T.; Burmester, G.R.; Dörner, T. The Diagnosis and Treatment of Sjögren's Syndrome. *Dtsch. Ärzteblatt Int.* **2017**, *114*, 354. [CrossRef]
2. Shiboski, C.H.; Shiboski, S.C.; Seror, R.; Criswell, L.A.; Labetoulle, M.; Lietman, T.M.; Rasmussen, A.; Scofield, H.; Vitali, C.; Bowman, S.J.; et al. 2016 American College of Rheumatology/European League Against Rheumatism Classification Criteria for Primary Sjögren's Syndrome: A Consensus and Data-Driven Methodology Involving Three International Patient Cohorts. *Arthritis. Rheumatol.* **2017**, *69*, 35–45. [CrossRef] [PubMed]
3. Jonsson, M.V.; Baldini, C. Major Salivary Gland Ultrasonography in the Diagnosis of Sjögren's Syndrome: A Place in the Diagnostic Criteria? *Rheum. Dis. Clin. N. Am.* **2016**, *42*, 501–517.
4. Pomorska, A.; Swie˛ton´, D.; Lieberman, S.M.; Bryl, E.; Kosiak, W.; Pe˛ksa, R.; Chora˛´ zewicz, J.; Kochan´ska, B.; Kowalska-Skabara, J.;˙ Szumera, M.; et al. Recurrent or persistent salivary gland enlargement in children: When is it Sjögren's? *Semin. Arthritis Rheum.* **2022**, *52*, 151945. [CrossRef] [PubMed]
5. Swiecka, M.; Mas´lin´ska, M.; Paluch, Ł.; Zakrzewski, J.; Kwiatkowska, B. Imaging methods in primary Sjögren's Syndrome as´ potential tools of disease diagnostics and monitoring. *Reumatologia/Rheumatology* **2019**, *57*, 336–342. [CrossRef] [PubMed]
6. Buus, S.; Grau, C.; Munk, O.L.; Bender, D.; Jensen, K.; Keiding, S. 11C-methionine PET, a novel method for measuring regional salivary gland function after radiotherapy of head and neck cancer. *Radiother. Oncol.* **2004**, *73*, 289–296. [CrossRef] [PubMed]
7. Takashima, S.; Takeuchi, N.; Morimoto, S.; Tomiyama, N.; Ikezoe, J.; Shogen, K.; Kozuka, T.; Okumura, T. MR Imaging of Sjögren Syndrome. *J. Comput. Assist. Tomogr.* **1991**, *15*, 393–400. [CrossRef]
8. Chu, C.; Feng, Q.; Zhang, H.; Zhu, Y.; Chen, W.; He, J.; Sun, L.; Zhou, Z. Whole-Volume ADC Histogram Analysis in Parotid Glands to Identify Patients with Sjögren's Syndrome. *Sci. Rep.* **2019**, *9*, 9614. [CrossRef]
9. Chu, C.; Wang, F.; Zhang, H.; Zhu, Y.; Wang, C.; Chen, W.; He, J.; Sun, L.; Zhou, Z. Whole-volume ADC Histogram and Texture Analyses of Parotid Glands as an Image Biomarker in Evaluating Disease Activity of Primary Sjögren's Syndrome. *Sci. Rep.* **2018**, *8*, 15387. [CrossRef]
10. Ganeshan, B.; Skogen, K.; Pressney, I.; Coutroubis, D.; Miles, K. Tumour heterogeneity in oesophageal cancer assessed by CT texture analysis: Preliminary evidence of an association with tumour metabolism, stage, and survival. *Clin. Radiol.* **2012**, *67*, 157–164. [CrossRef]
11. Chen, P.; Dong, B.; Zhang, C.; Tao, X.; Wang, P.; Zhu, L. The histogram analysis of apparent diffusion coefficient in differential diagnosis of parotid tumor. *Dentomaxillofacial. Radiol.* **2020**, *49*, 20190420. [CrossRef]
12. Tonami, H.; Higashi, K.; Matoba, M.; Yokota, H.; Yamamoto, I.; Sugai, S. A Comparative Study Between MR Sialography and Salivary Gland Scintigraphy in the Diagnosis of Sjögren Syndrome. *J. Comput. Assist. Tomogr.* **2001**, *25*, 262–268. [CrossRef]
13. Tustison, N.J.; Avants, B.B.; Cook, P.A.; Zheng, Y.; Egan, A.; Yushkevich, P.A.; Gee, J.C. N4ITK: Improved N3 bias correction. *IEEE Trans. Med. Imaging* **2010**, *29*, 1310e20. [CrossRef] [PubMed]
14. Pyradiomics Organization. Pyradiomics Documentation. 2019. Available online: https://pyradiomics.readthedocs.io/en/latest/ (accessed on 1 April 2023).
15. Castellano, G.; Bonilha, L.; Li, L.M.; Cendes, F. Texture analysis of medical images. *Clin. Radiol.* **2004**, *59*, 1061e9. [CrossRef] [PubMed]
16. Kalk, W.W.; Vissink, A.; Spijkervet, F.K.; Bootsma, H.; Kallenberg, C.G.; Roodenburg, J.L. Parotid sialography for diagnosing Sjögren syndrome. *Oral Surg. Oral Med. Oral Pathol. Oral Radiol. Endod.* **2002**, *94*, 131–137. [CrossRef] [PubMed]
17. Ng, F.; Ganeshan, B.; Kozarski, R.; Miles, K.A.; Goh, V. Assessment of primary colorectal cancer heterogeneity by using whole-tumor texture analysis: Contrast-enhanced CT texture as a biomarker of 5-year survival. *Radiology* **2013**, *266*, 177–184. [CrossRef]
18. Márton, K.; Boros, I.; Fejérdy, P.; Madléna, M. Evaluation of unstimulated flow rates of whole and palatal saliva in healthy patients wearing complete dentures and in patients with Sjogren's Syndrome. *J. Prosthet. Dent.* **2004**, *91*, 577–581. [CrossRef]
19. Tzioufas, A.G.; Moutsopoulos, H.M. Salivary gland imaging techniques for the diagnosis of Sjögren's Syndrome. *Int. J. Clin. Rheumtol.* **2009**, *4*, 321–327. [CrossRef]
20. Makanyanga, J.; Ganeshan, B.; Rodriguez-Justo, M.; Bhatnagar, G.; Groves, A.; Halligan, S.; Miles, K.; Taylor, S.A. MRI texture analysis (MRTA) of T2-weighted images in Crohn's disease may provide information on histological and MRI disease activity in patients undergoing ileal resection. *Eur. Radiol.* **2017**, *27*, 589. [CrossRef]

21. de Figueiredo, E.H.; Borgonovi, A.F.; Doring, T.M. Basic Concepts of MR Imaging, Diffusion MR Imaging, and Diffusion Tensor Imaging. Magn. Reason. *Imaging Clin. N. Am.* **2011**, *19*, 1–22. [CrossRef]
22. Cohen, J.; Cohen, P.; West, S.G.; Aiken, L.S. *Applied Multiple Regression/Correlation Analysis for the Behavioral Sciences*, 3rd ed.; Lawrence Erlbaum Associates, Inc.: Mahwah, NJ, USA, 2003.
23. Cho, S.H.; Kim, G.C.; Jang, Y.-J.; Ryeom, H.; Kim, H.J.; Shin, K.-M.; Park, J.S.; Choi, G.-S.; Kim, S.H. Locally advanced rectal cancer: Post-chemoradiotherapy ADC histogram analysis for predicting a complete response. *Acta Radiol.* **2015**, *56*, 1042–1050. [CrossRef] 24. Zhong, W.; Zhang, H.; Ran, H. Advances in imaging of the lacrimal gland in Sjögren's Syndrome: A narrative review. *J. Clin. Ultrasound* **2023**, 1–10. [CrossRef]
25. Muntean, D.D.; Bădărînză, M.; S¸tefan, P.A.; Lenghel, M.L.; Rusu, G.M.; Csutak, C.; Coroian, P.A.; Lupean, R.A.; Fodor, D. The Diagnostic Value of MRI-Based Radiomic Analysis of Lacrimal Glands in Patients with Sjögren's Syndrome. *Int. J. Mol. Sci.* **2022**, *23*, 10051. [CrossRef]
26. Freni, F.; Gazia, F.; D'alcontres, F.S.; Galletti, B.; Galletti, F. Use of botulinum toxin in Frey's syndrome. *Clin. Case Rep.* **2019**, *7*, 482–485. [CrossRef]
27. Furness, S.; Bryan, G.; McMillan, R.; Worthington, H.V. Interventions for the Management of Dry Mouth: Non-Pharmacological Interventions. In *Cochrane Database of Systematic Reviews*; Furness, S., Ed.; John Wiley & Sons, Ltd.: Chichester, UK, 2013.
28. Hammenfors, D.S.; Valim, V.; Bica, B.E.R.G.; Pasoto, S.G.; Lilleby, V.; Nieto-González, J.C.; Silva, C.A.; Mossel, E.; Pereira, R.M.R.; Coelho, A.; et al. Juvenile Sjögren's Syndrome: Clinical Characteristics with Focus on Salivary Gland Ultrasonography. *Arthritis. Care Res.* **2020**, *72*, 78–87. [CrossRef]